

Unraveling Organocuprate Complexity: Fundamental Insights into Intrinsic Group Transfer Selectivity in Alkylation Reactions^ξ

Nicole J. Rijs,^{a,b,ψ} Naohiko Yoshikai,^c Eiichi Nakamura^d and Richard A. J. O'Hair^{a,b}*

(a) School of Chemistry and Bio21 Institute of Molecular Science and Biotechnology, The University of Melbourne, Victoria 3010, Australia. E-mail: rohair@unimelb.edu.au

(b) ARC Centre of Excellence for Free Radical Chemistry and Biotechnology.

(c) Division of Chemistry and Biological Chemistry, School of Physical and Mathematical Sciences, Nanyang Technological University, Singapore 637371. E-mail: nyoshikai@ntu.edu.sg

(d) Department of Chemistry, The University of Tokyo, Bunkyo-ku, Tokyo 113-0033, Japan. E-mail: nakamura@chem.s.u-tokyo.ac.jp

ξ Dedicated to Prof. John Bowie, on the occasion of his 75th Birthday.

ψ Currently at: Institut für Chemie, Technische Universität Berlin, Straße des 17. Juni 115, 10623 Berlin, Germany.

* Corresponding Author: Phone +61 3 8344-2452; FAX: +61 3 9347-5180

EMAIL rohair@unimelb.edu.au

RECEIVED DATE

TITLE RUNNING HEAD: Group Transfer Selectivity in Reactions of $[\text{CH}_3\text{CuR}]^-$ with Methyl Iodide.

Abstract

The intrinsic gas-phase reactivity and selectivity of alkylation reactions between a series of well-defined mixed organocuprate anions and methyl iodide were examined. The series $[\text{CH}_3\text{CuR}]^-$ (where R = CH_3CH_2 , $\text{CH}_3\text{CH}_2\text{CH}_2$, $(\text{CH}_3)_2\text{CH}$, PhCH_2CH_2 , PhCH_2 , Ph or C_3H_5), and $[\text{CH}_3\text{CuH}]^-$ were allowed to undergo ion-molecule reactions with CH_3I under the near thermal conditions of an ion-trap mass spectrometer. The rates of reaction (reaction efficiencies) and the product ion branching ratios (selectivities) were compared with those of the reaction between dimethylcuprate and CH_3I , and were found to be influenced by the nature of R. Alkyl R groups yielded similar reaction efficiencies, however they showed a selectivity for C-C bond formation at the coordinated R group. Inclusion of unsaturated R groups curbed the overall reactivity, yielding reaction efficiencies 1 to 2 orders of magnitude lower. With the exception of R = PhCH_2CH_2 , these switched their selectivity to C-C bond formation at the CH_3 group. Replacing an organyl ligand with R = H significantly enhanced the reactivity by 8 times and resulted in the selective formation of methane. Unique decomposition and side-reactions were observed for certain ligands, e.g. (1) evidence of spontaneous β -hydride elimination from $[\text{RCu}]^-$ byproducts; and (2) homo-coupling of the pre-existing organocuprate ligands in $[\text{CH}_3\text{CuC}_3\text{H}_5]^-$, as shown by deuterium labeling. DFT calculations (B3LYP-D/Def2-QZVP//B3LYP/SDD:6-31+G(d)) predict the favored alkylation mechanism for all species is via an oxidative addition/reductive elimination (OA/RE) pathway. OA is the rate limiting step, while RE determines selectivity. The role of R in altering the observed reactivity is examined.

Keywords: alkylation, mixed organocuprates, selectivity, DFT, mass spectrometry, ion-molecule reaction, methyl iodide, oxidative addition, cross-coupling, organometallic, gas-phase.

Introduction

Organocuprate coupling reactions remain one of the workhorses of organic synthesis.¹ Corey and Posner first reported stoichiometric reactions between cuprates and a range of organic substrates in the late 1960s in their classic exploration of the C-C coupling reactions of Gilman reagents, R_2CuLi .²

It was recognized that a homocuprate reagent R_2CuLi can only effectively transfer a single R group to an electrophilic substrate. The other one is “wasted” as an RCu byproduct. In order to overcome this issue of poor atom economy,³ especially where the R group is synthetically “precious”, Corey and Beames subsequently introduced the concept of hetero (or mixed) organocuprate reagents,⁴ $R'RCuLi$, in which the R' group is unreactive and remains bound, thus behaving as a non-transferable “dummy ligand”.⁵ Their initial report focused on the use of $R' =$ cyclopentadienyl and acetylide.⁵ Subsequent studies by the groups of House, Whitesides, Posner and Corey established the following selectivity orders for the intramolecular ligand transfer reactions of mixed diorganocuprates: $n-Bu \approx sec-Bu > t-Bu$; $Ph > alkynyl$; and $alkenyl > CH_3 > alkynyl$.⁶ Since then, the dummy ligand approach has been extended to synthetically useful heterocuprates containing the following other non-transferable ligands: cyano,^{7a} phenylthio,^{7b} alkoxy,^{7c} dialkylamino,^{7d,e} phosphido,^{7d,e} and trimethylsilylmethyl.^{7e,f}

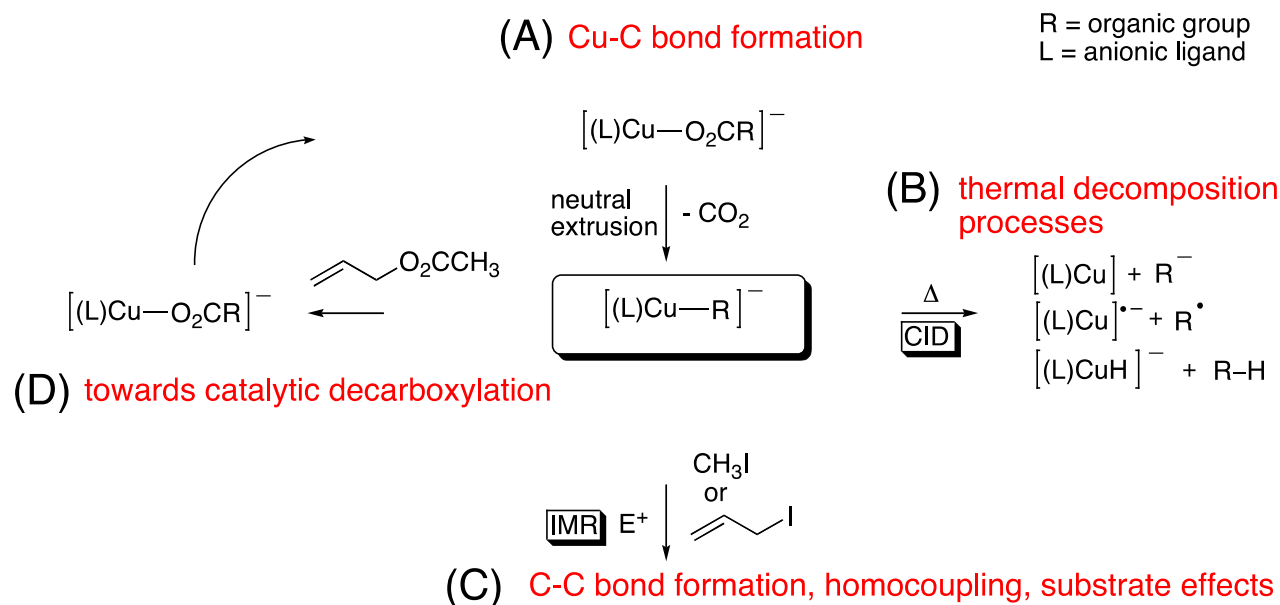
Despite the synthetic utility of mixed diorganocuprates and recent kinetic studies of their reactions with alkyl halides,⁸ these reagents suffer from what Bertz et al. have described as “Organocuprate Complexity”.⁹ Thus the interplay of: the nucleophilic copper reagent (e.g. structure, nature of the dummy ligand (R'), cluster size, overall charge etc), the electrophilic organic substrate and the reaction medium (solvent, counter ions etc) in controlling reaction pathways remain poorly understood. Indeed for some time a controversy raged around the binding site of the cyanide anion in one of the most

popular classes of organocuprates, the “higher order” cyanocuprates.¹⁰ Lipshutz and co-workers initially postulated the formation of so-called higher-order diorganocuprates $\text{Li}_2\text{CuR}_2(\text{CN})$, in which the CN^- ions coordinate to the Cu centers.¹⁰ This was challenged by several groups, who used ^{13}C NMR and X-ray absorption spectroscopic measurements as well as theoretical calculations to propose the existence of lower-order diorganocuprates $\text{LiCuR}_2\cdot\text{LiCN}$, which resemble traditional Gilman-type cuprates in which the CN^- is coordinated to Li^+ instead.¹¹ The lower-order nature of Lipshutz-type cyanocuprates was subsequently confirmed from X-ray crystal structures.^{11ij} Despite this closure on the structural controversy of cyanocuprates,¹² their aggregation state continues to receive attention, with electrospray ionization mass spectrometry providing some valuable insights.¹³ Importantly, this narrative highlights the need for well-defined experimental studies that can examine the intrinsic properties of organocuprate reagents. Ideally these studies should reduce the complexity, have a systematic approach and exquisite control over the experimental parameters. Experimental gas-phase studies and/or electronic structure calculations provide a powerful way of uncovering both the intrinsic reactivity of organometallic species and the mechanisms of metal-mediated C-C bond coupling reactions in this manner.¹⁴⁻¹⁸ Previous studies on the intrinsic gas-phase reactivity of organocuprates have focused on understanding:

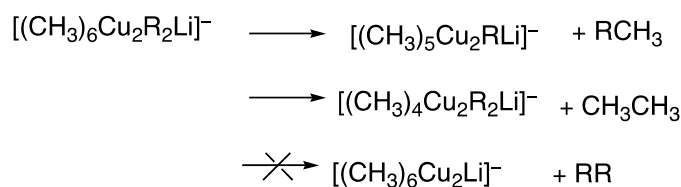
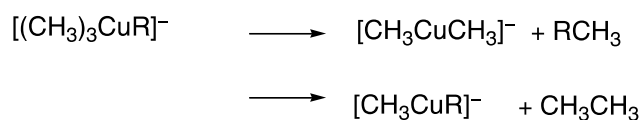
- (i) The mechanism of formation and successful generation of homo-, hetero- and mixed diorganocuprates from copper carboxylate precursors (Scheme 1, A).¹⁹
- (ii) The thermal decomposition processes of homo- and mixed diorganocuprates (Scheme 1, B).^{20,21}
- (iii) Bimolecular alkylation^{20c,22} and allylation²³ reactions with homocuprates (Scheme 1, C), to uncover substrate effects.
- (iv) The requirements to develop a catalytic cycle for the decarboxylative allylation of $[\text{CH}_3\text{CuCH}_3]^-$ with allyl acetate (Scheme 1, D).²⁴
- (v) The comparison of the above reactions to the heavier Group 11 congeners of the organometallates and metal center effects.^{19b,20-23}

- (vi) The key reductive elimination step for Cu(III) tetraorganocuprates, $[(\text{CH}_3)_3\text{CuR}]^-$, and the triple ions $[(\text{CH}_3)_6\text{Cu}_2\text{R}_2\text{Li}]^-$ (Scheme 1, E).²⁵

Scheme 1. Intrinsic properties of gas-phase organocuprate anions previously explored.



(E) reductive elimination from Cu(III) species



Two theoretical studies have also systematically examined ligand effects in conjugate addition reactions of heterocuprates.²⁶ Three different model systems were used to consider the role of the ligand in C-C bond formation:

- (i) A simple model Cu(III) complex, $(\text{CH}_3)_2(\text{X})\text{Cu}(\text{III})\text{O}(\text{CH}_3)_2$; to examine the activation energy of the reductive elimination step of $\text{X}-\text{CH}_3$.^{26a} The activation energies for reductive elimination of $\text{X}-\text{CH}_3$ was found to follow the order: $\text{CH}=\text{CH}_2 < \text{C}\equiv\text{CH} < \text{C}\equiv\text{N} < \text{CH}_2\text{Si}(\text{CH}_3)_3 < \text{CH}_3 < \text{N}(\text{CH}_3)_2 < \text{SCH}_3$.
- (ii) A π -allyl Cu(III) model, $\text{CH}_3(\text{X})\text{Cu}(\eta^3\text{-C}_3\text{H}_5)$; to compare the activation energies for the competing reductive elimination of $\text{CH}_3\text{-C}_3\text{H}_5$ and $\text{X-C}_3\text{H}_5$.^{26b} Reductive elimination of $\text{CH}_3\text{-C}_3\text{H}_5$ was found to be preferred over that of $\text{X-C}_3\text{H}_5$ for the dummy ligands; $\text{X} = \text{C}\equiv\text{CH}$, $\text{C}\equiv\text{N}$, SCH_3 , and $\text{CH}_2\text{Si}(\text{CH}_3)_3$. In contrast, reductive elimination of an alkenyl group is less energetically demanding than that of a methyl group. The ligand transfer selectivity for $\text{X} = \text{C}\equiv\text{CH}$, $\text{C}\equiv\text{N}$, and SCH_3 was ascribed to their weaker σ -donation ability, compared to that of CH_3 , which influences the geometry associated with the reductive elimination process.
- (iii) The cluster $\text{CH}_3(\text{X})\text{CuLi}\cdot\text{LiCl}$ with acrolein; to examine the complete potential energy diagram for competing C-X and C-CH_3 bond formation.^{26b} Key factors that influence the preferential formation of the C-CH_3 bond are (1) a strong X-Li bond and (2) the trans effect of X , both of which assist the X group to remain attached to Cu .

Here we use gas-phase mass spectrometry experiments to examine the intrinsic effects of ligands on reactivity and selectivity of alkylation reactions between the well-defined mixed diorganocuprates, $[\text{CH}_3\text{CuR}]^-$ or methyl copper hydride $[\text{CH}_3\text{CuH}]^-$ (Scheme 2, **1-4**, **6-10**) and the electrophile methyl iodide. Electronic structure calculations are subsequently used to examine any observed differences in reactivity and selectivity as a function of R for the alkylation reaction with $[\text{CH}_3\text{CuR}]^-$ (Scheme 2, **1-10**).

Scheme 2. Well-defined $[\text{CH}_3\text{CuR}]^-$ reagent ions systematically examined in this report; experimentally (1-4, 6-10) and theoretically (1-10). The m/z values refer to complexes containing the ^{63}Cu isotope.

entry	R =	m/z	structure
1	CH_3	93	$[\text{CH}_3\text{Cu}-\text{CH}_3]^-$
2	CH_3CH_2	107	$[\text{CH}_3\text{Cu}-\text{CH}_2\text{CH}_3]^-$
3	$\text{CH}_3\text{CH}_2\text{CH}_2$	121	$[\text{CH}_3\text{Cu}-\text{CH}_2\text{CH}_2\text{CH}_3]^-$
4	$(\text{CH}_3)_2\text{CH}$	121	$[\text{CH}_3\text{Cu}-\text{CH}(\text{CH}_3)_2]^-$
5	$(\text{CH}_3)_3\text{C}$	n/a	$[\text{CH}_3\text{Cu}-\text{C}(\text{CH}_3)_3]^-$
6	PhCH_2CH_2	119	$[\text{CH}_3\text{Cu}-\text{CH}_2\text{CH}_2\text{Ph}]^-$
7	PhCH_2	183	$[\text{CH}_3\text{Cu}-\text{CH}_2\text{Ph}]^-$
8	Ph	169	$[\text{CH}_3\text{Cu}-\text{Ph}]^-$
9	C_3H_5	155	$[\text{CH}_3\text{Cu}-\text{CH}_2\text{CH}=\text{CH}_2]^-$
10	H	79	$[\text{CH}_3\text{Cu}-\text{H}]^-$

Experimental

Reagents. Methyl iodide, d_3 -methyl iodide, copper(II) acetate, vinyl acetic acid and hydrocinnamic acid were obtained from Aldrich. Propionic acid, phenyl acetic acid and n-butyric acid were obtained from BDH Laboratory Supplies. Isobutyric acid and methanol were obtained from Ajax. Benzoic acid was obtained from May Baker. All chemicals were used without further purification.

Mass Spectrometry. A modified Finnigan LCQ quadrupole ion trap mass spectrometer equipped with a Finnigan electrospray ionization (ESI) source was used to generate and study the gas-phase ion-molecule reactions of mixed organocuprates. The modification of the instrument and the formation of

the mixed Cu(I) carboxylates $[\text{CH}_3\text{CO}_2\text{CuO}_2\text{CR}]^-$ have been extensively described previously.^{19,27} Methanolic solutions of copper(II) acetate and the appropriate carboxylic acid (0.5-1 mM, in a 1:2 molar ratio) were infused into the ESI source via a syringe pump operating at a flow rate of 5 $\mu\text{L}/\text{min}$. The electrospray source typically operated at needle potentials of 3.5–4.5 kV and a heated capillary temperature of 180°C. The ‘advanced scan’ function of the LCQ software was used for mass selection, subsequent collisional activation (CID) and ion-molecule reactions (IMR). $[\text{CH}_3\text{CuH}]^-$ was generated from $[\text{CH}_3\text{CuCH}_2\text{CH}_3]^-$ by an extra CID step as described previously.^{20b} Ion-molecule kinetic measurements were carried out by introducing methyl iodide into the ion trap via the helium inlet line and then measuring the decay of the mass selected reactant organocuprate, $[\text{CH}_3\text{CuR}]^-$ (1-4, 6-10, Scheme 2), over a range of reaction times. The intensity of the reactant ion was calculated by integration of its ion count within the mass-selected window. Extrapolation of plots of $-\ln([\text{CH}_3\text{CuR}]^- \text{ intensity}/\text{total ions})$ vs. the reaction time gave *pseudo* first-order rates, which were converted to rate constants by dividing the *pseudo* first-order rate coefficient by the calculated concentration of methyl iodide in the ion trap. The rate constants reported are the average of at least 3 independent measurements conducted on at least 3 separate days.²⁸ Standard deviations in rate constants were typically around 5-10%. A conservative estimate of error is $\pm 25\%$, but relative rates are expected to be more accurate due to cancellation of errors. Collision rates (k_{ADO}) for reaction efficiencies were calculated via the Average Dipole Orientation (ADO) theory of Su and Bowers using the COLRATE program.²⁹

Electronic Structure Calculations. Theoretical calculations were carried out to provide insights into the bimolecular reactivity of the organocuprate anions with methyl iodide. Geometry optimizations and vibrational frequency calculations were carried out with the Gaussian 09 suite of programs,³⁰ using the B3LYP hybrid functional.³¹ The Stuttgart Dresden (SDD) basis set and effective core potential (ECP) were used for the copper and iodine atoms while the 6-31+G(d) all electron basis set was used for carbon and hydrogen.³² This combination was chosen: (i) since it has been shown to be effective in

calculating organometallate structures while being less demanding than higher levels of *ab initio* theory;³³⁻³⁴ (ii) to allow structural comparison with previous work.^{20c,23,24} The optimized B3LYP geometry of the dimethylcuprate anion has been shown to be in excellent structural agreement to that determined from X-ray crystallography.^{20a,20c} All transition state (TS) geometries were characterized by the presence of a single imaginary frequency and intrinsic reaction coordinates (IRC) were examined to ensure smooth connection of reactants and products. Single point energies previously calculated with successively more complete basis sets showed that these did not alter the relative ordering of predicted energetic pathways.²³ Energetics presented were calculated with B3LYP utilizing the Def2-QZVP basis set (C, H = all electron; Cu and I = incl. ECP)^{35a-c} and Grimme's D2 empirical dispersion,^{35d} defined as B3LYP-D/Def2-QZVP//B3LYP/SDD:6-31+G(d). All quoted relative energies (E_0) include zero point vibrational energy (unscaled) calculated at the optimization level, without correction for basis set superposition error.

To assess the robustness of the B3LYP results, single point energies at key stationary points were calculated with the M06 functional^{36a} and the B2PLYP-D double hybrid functional^{36b,c}, along with B3LYP³¹ (Supporting Information, Table S1-S4). While there is some lowering in the value of the relative energies using methods that account for dispersion, particularly with respect to the TSs for reductive elimination, in this work the predicted energetic trends are consistent between all four methods (B3LYP-D, M06, B2PLYP-D and B3LYP). Thus, due to this agreement, we are confident of the trends we wish to discuss here and draw on all of these results.

Visualizations of the molecules appearing in this report were created using MacMolPlt.³⁷

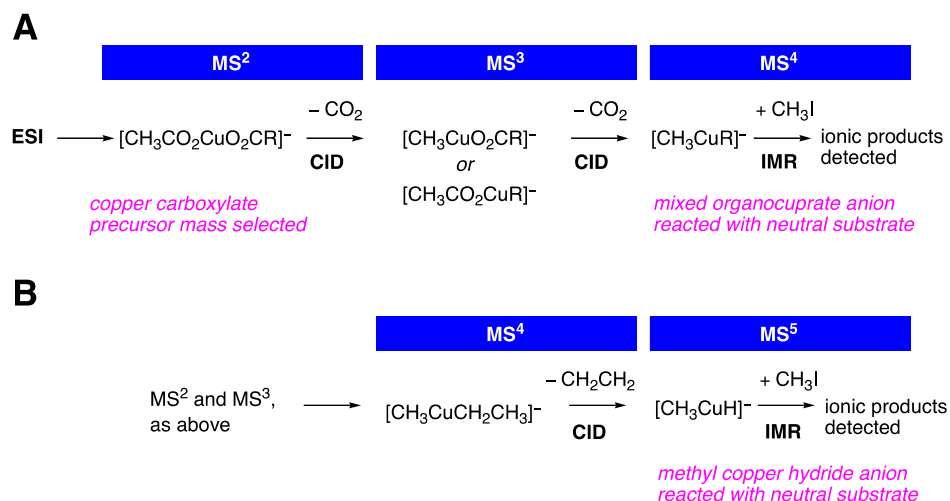
Results and Discussion

1.0 Intrinsic reactivity: methyl iodide with mixed organocuprates, [CH₃CuR]⁻.

The diorganocuprate precursor ions (Scheme 2) were generated via multistage mass spectrometry methods using sequential CID steps to induce decarboxylation reactions of the copper carboxylate anions generated via electrospray ionization.³⁸⁻⁴⁰ Since these reactions have been previously described

in detail, they are only summarized in Scheme 3, A.¹⁹ The copper hydride (**10**, Scheme 2) was formed via the previously described β -hydride elimination reaction (Scheme 3, B).^{20b,41} The bimolecular ion-molecule reactions of the organocuprates with methyl iodide (representing a series of MS⁴ experiments, and **10** MS⁵, Scheme 3), were carried out under the near thermal conditions of the quadrupole ion trap.^{28b} Figure 1 shows representative ion-molecule reactions of the mixed organocuprate anions [CH₃CuR]⁻ (**3**, **7**, **8** and **10**, Scheme 2) while Table 1 lists the rates, reaction efficiencies and product branching ratios for the ion-molecule reactions of all the organocuprates experimentally examined (**1-4**, **6-10**, Scheme 2). We note that **5** was not examined experimentally due to the inability of the double-decarboxylation strategy to generate this ion.^{19a}

Scheme 3. Experimental strategy using ESI coupled with multistage mass spectrometry experiments, MSⁿ, to allow the gas-phase generation and the study of the reaction with methyl iodide of: (A) mixed-organocuprate anions [CH₃CuR]⁻; (B) methyl(hydrido)cuprate anions [CH₃CuH]⁻.



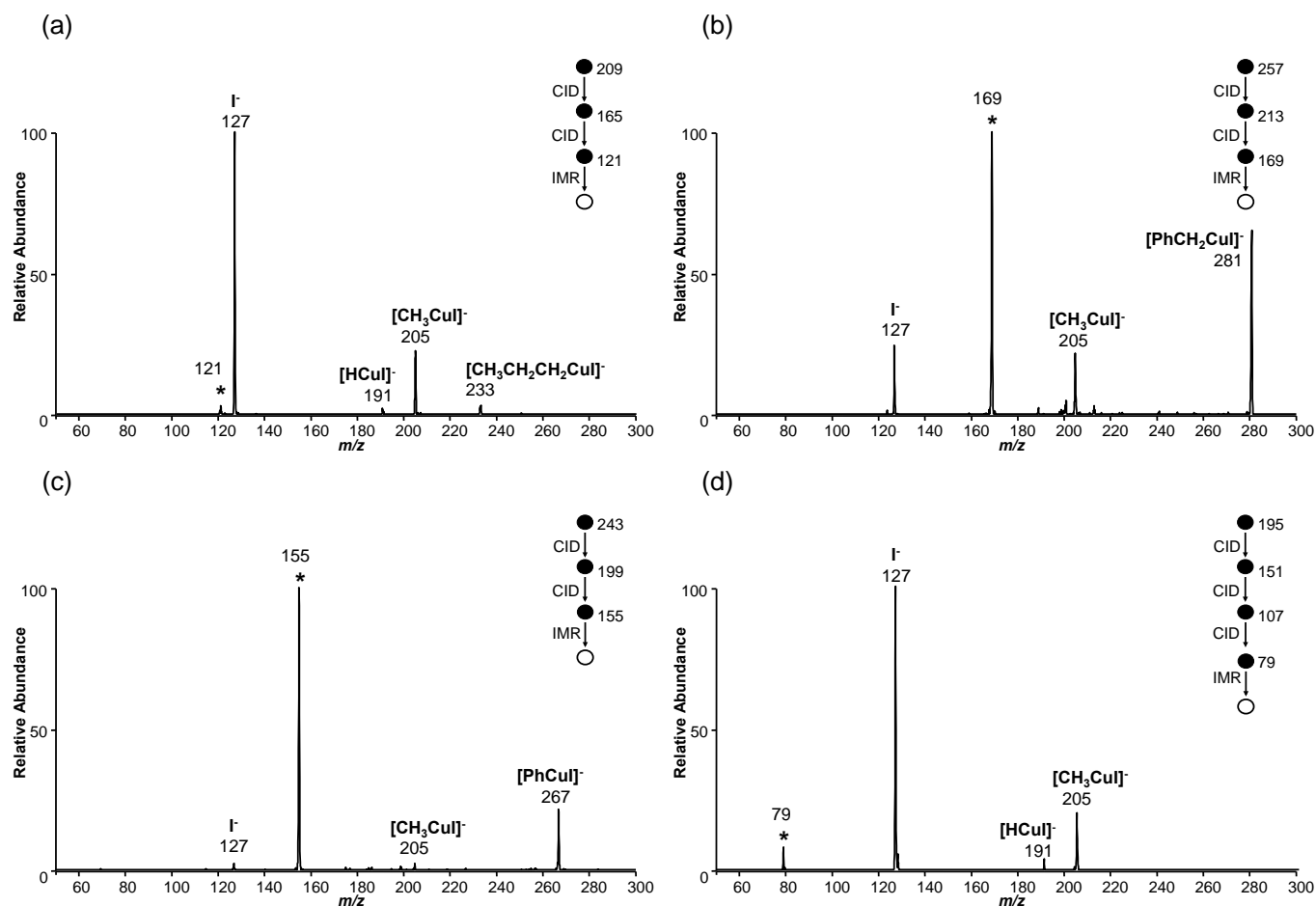


Figure 1. Mass spectra showing the ion-molecule reaction between, methyl iodide, CH_3I and the mass selected mixed organocuprate anions $[CH_3CuR]^-$, (a) **8**, $R = CH_3CH_2CH_2$ (m/z 121); (b) **7**, $R = PhCH_2$ (m/z 169); (c) **8**, $R = Ph$ (m/z 155); (d) **10**, $R = H$ (m/z 79). The mass-selected ion is marked with an * in each case and the MS^n approach used is given in Scheme 3.

An examination of Figure 1 reveals the formation of three primary product ions: $[CH_3CuI]^-$ (m/z 205), $[RCuI]^-$ and I^- (m/z 127). The organometallic ions $[CH_3CuI]^-$ and $[RCuI]^-$ arise from C-C bond cross-coupling reactions at the R and CH_3 groups respectively (eqs 1 and 2). Since we do not detect the neutral compound(s) formed, the observed iodide product, I^- , could arise from three possible reactions: (i) formation of the combined neutral products RCH_3 and CH_3Cu (eq. 3); (ii) formation of the combined neutral products CH_3CH_3 and RCu (eq. 4); (iii) formation of the neutral copper(III) species $[(CH_3)_2CuR]$ (eq. 5). The latter possibility seems unlikely in light of poor stability of neutral organocopper(III)

species.⁴² For R groups containing β -hydrogens, the secondary product ion $[\text{HCuI}]^-$ is often observed (e.g. Figure 1a, m/z 191). This arises as a consequence of the exothermic C-C bond coupling reaction, which produces “hot” $[\text{RCuI}]^-$ which can either undergo collisional cooling with the He bath gas or undergo β -hydride elimination (eq. 6). Another pathway, β -group elimination (eq. 7) is available for **3** and **6**, where the β -organyl group, $X = \text{CH}_3$ or Ph respectively, is transferred. However this pathway is obscured for **3** and only trace amounts are observed for **6**.⁴³

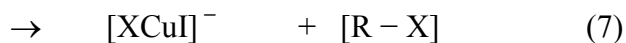
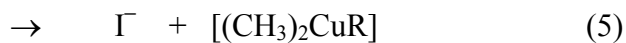
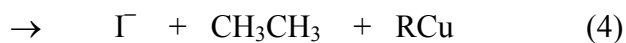
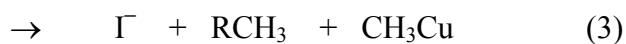
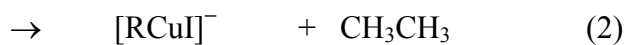


Table 1. Experimentally derived kinetics and branching ratios of ionic products for the gas-phase ion-molecule reactions of methyl iodide with the mixed organocuprate anions $[\text{CH}_3\text{CuR}]^-$ (Scheme 2).

		rate data		% product ion branching ratios				
R =	$k_{\text{measured}}^{(a),(b)}$	efficiency ^(c)	Γ^-	$[\text{CH}_3\text{CuI}]^-$	$[\text{RCuI}]^-$	$[\text{HCuI}]^-$	$[\text{XCuI}]^-^{(d)}$	
1 ^(e) CH ₃	3.77 ± 0.37	3	73	27	27	(f)	(f)	
2 CH ₃ CH ₂	5.27 ± 0.45	4	85	13	1	1	(f)	
3 CH ₃ CH ₂ CH ₂	3.05 ± 0.15	3	74	21	4	2	(g)	
4 (CH ₃) ₂ CH	4.19 ± 0.24	4	90	8	2	1	(f)	
6 PhCH ₂ CH ₂	0.440 ± 0.4 0.0083		34	45	20	1	<1	
7 PhCH ₂	0.0290 ± 0.03 0.0023		15	23	62	(f)	(f)	
8 Ph	0.0102 ± 0.01 0.00024		8	11	81	0	(f)	
9 C ₃ H ₅	0.246 ± 0.2 0.053		61	15	21	3	(f)	
10 H	31.2 ± 3.7	24	82	17	1	(f)	(f)	

(a) in units of $10^{-11} \text{ cm}^3 \cdot \text{molecules}^{-1} \cdot \text{s}^{-1}$

(b) errors are one standard deviation

(c) %, where reaction efficiency = $((k_{\text{measured}}/k_{\text{ADO}}) \times 100)$

(d) where X = β -group other than hydrogen (eq. 7)

(e) the experimental values found for this work reproduced the previously reported experimental values found in reference 22.

(f) not applicable

(g) reaction channel overlaps cross-coupling channel (i.e. $[\text{CH}_3\text{CuI}]^-$)

An examination of Table 1 reveals that the gas-phase rates of the reaction, reaction efficiencies and the product branching ratios are indeed influenced by the nature of the organyl ligand, R (Scheme 2). All of the organocuprate species examined here show an appreciable reaction under the experimental conditions. The observed reaction efficiencies range from 0.01% to 24%. The alkyl(methyl)cuprates **2** - **4** (R = CH₃CH₂, CH₃CH₂CH₂, or (CH₃)₂CH) are essentially as reactive as dimethylcuprate **1** in this

reaction (3-4% efficiency). However, they show a preference for C-C bond coupling at the R group (eq. 1) over the CH₃ group (eq. 2), the former and the latter having branching ratios of 8-21% and 1-4%, respectively. Thus, these organocuprate species are selective for RCH₃ formation (eq. 1). The non-aliphatic R groups (**6** - **9**) have a dramatic influence on the overall reactivity when compared to dimethylcuprate (**1**), their inclusion yielding reaction efficiencies lower by 1 to 2 orders of magnitude. The efficiencies follow the order: Ph < PhCH₂ << C₃H₅ < PhCH₂CH₂. For the cuprates **7** - **9**, C-C bond coupling at the CH₃ group (eq. 2) is preferred to that at the R group (eq. 1). On the other hand, the phenethyl(methyl)cuprate **6** prefers formation of RCH₃ (eq. 1) as is the case with other alkyl(methyl)cuprates (**2** - **4**). Finally, when R = H (**10**), the reactivity is substantially enhanced compared to that of **1**, the reaction efficiency being 8 times higher, with a preference for C-H bond coupling (eq. 1). Thus the overall gas-phase reaction efficiencies for the reaction of [CH₃CuR]⁻ + CH₃I follow the order: Ph < PhCH₂ << C₃H₅ < PhCH₂CH₂ << CH₃CH₂CH₂ = CH₃ < (CH₃)₂CH = CH₃CH₂ << H.

We have recently shown that the reaction of dimethylcuprate with allyl iodide can proceed via a η³-allyl complex that can undergo competitive homo- and cross-coupling.²³ Thus it was of interest to establish whether a related π-allyl complex might be formed in reaction of [CH₃CuC₃H₅]⁻ (**9**) with methyl iodide. To examine this, we have studied the reaction of **9** [CH₃CuC₃H₅]⁻ with both CH₃I (Figure 2a) and CD₃I (Figure 2b). A comparison of these reactions with CH₃I versus CD₃I reveals that there is a minor formation of the homo-coupling product (Fig 2b, [CD₃CuI]⁻, *m/z* 208), which results from the direct coupling of the CH₃ and C₃H₅ ligands originating from the initial organocuprate reactant species. This allows us to infer some isomerization of the allyl group to a higher denticity ligation (i.e. a π-allyl system).²³

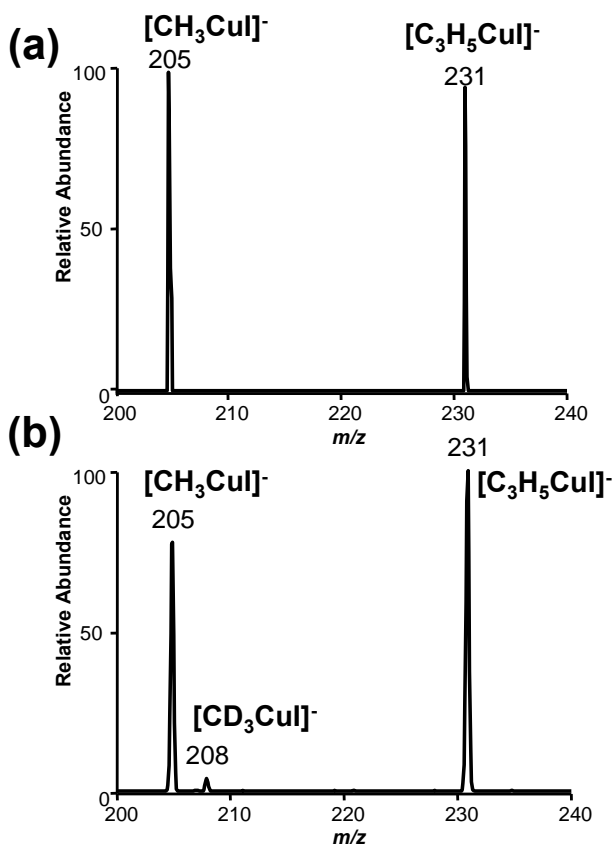


Figure 2. MS⁴ mass spectra showing the ion-molecule reaction between the mass selected methyl(allyl)cuprate anion [CH₃CuC₃H₅]⁻ (*m/z* 231, **9**) and: (a) methyl iodide, CH₃I; (b) d₃-methyl iodide, CD₃I. The region showing the C-C coupling channels is shown.

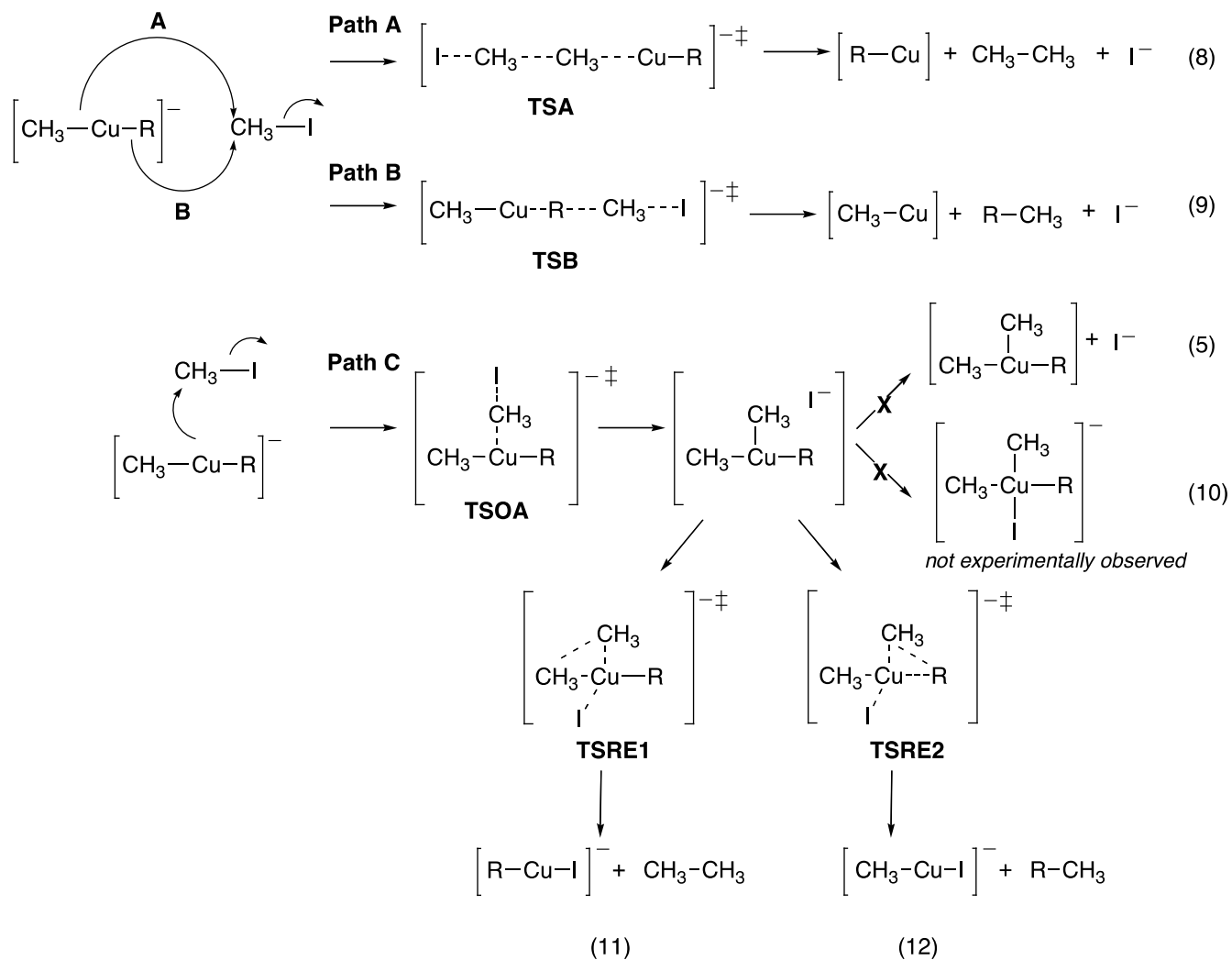
These experimental results clearly show that changing the organic group R of the organocuprate, [CH₃CuR]⁻, alters both the reactivity and the selectivity of the subsequent coupling reaction. The selectivity is reversed (from preferring R to CH₃) when alkyl ligands are replaced with unsaturated groups such as benzyl, phenyl, and allyl groups. These latter groups also significantly diminish the overall reactivity, as shown by their experimentally determined reaction efficiencies. In contrast, when a hydride replaces the organic group, there is a dramatic increase in the observed reaction rate. To help understand the origin of these differences in both reactivity and selectivity, we next discuss DFT predictions of the mechanisms that may operate in these C-C or C-H coupling reactions.

2.0 DFT predicted insights into ligand effects in the coupling reactions of methyl iodide organocuprates

Several coupling pathways were considered based on previous studies of nucleophilic organocuprate anions reacting with various electrophiles.^{20c,23,24} In particular, we have examined the following mechanistic scenarios: (1) concerted nucleophilic substitution (via an S_N2 type TS) from either of the non-equivalent α -carbons of the CH₃ or R ligands (Scheme 4, Path A and B; eqs 8 and 9); or (2) a stepwise oxidative addition (OA) followed by a reductive elimination (RE) at one of the two ligand sites (Scheme 4, Path C, eqs 11 and 12). The role of I⁻ was also explored by calculation of intermediates, TSs and products with and without the presence of iodine. The latter were higher in energy in every case (Supporting Information, Table S5).

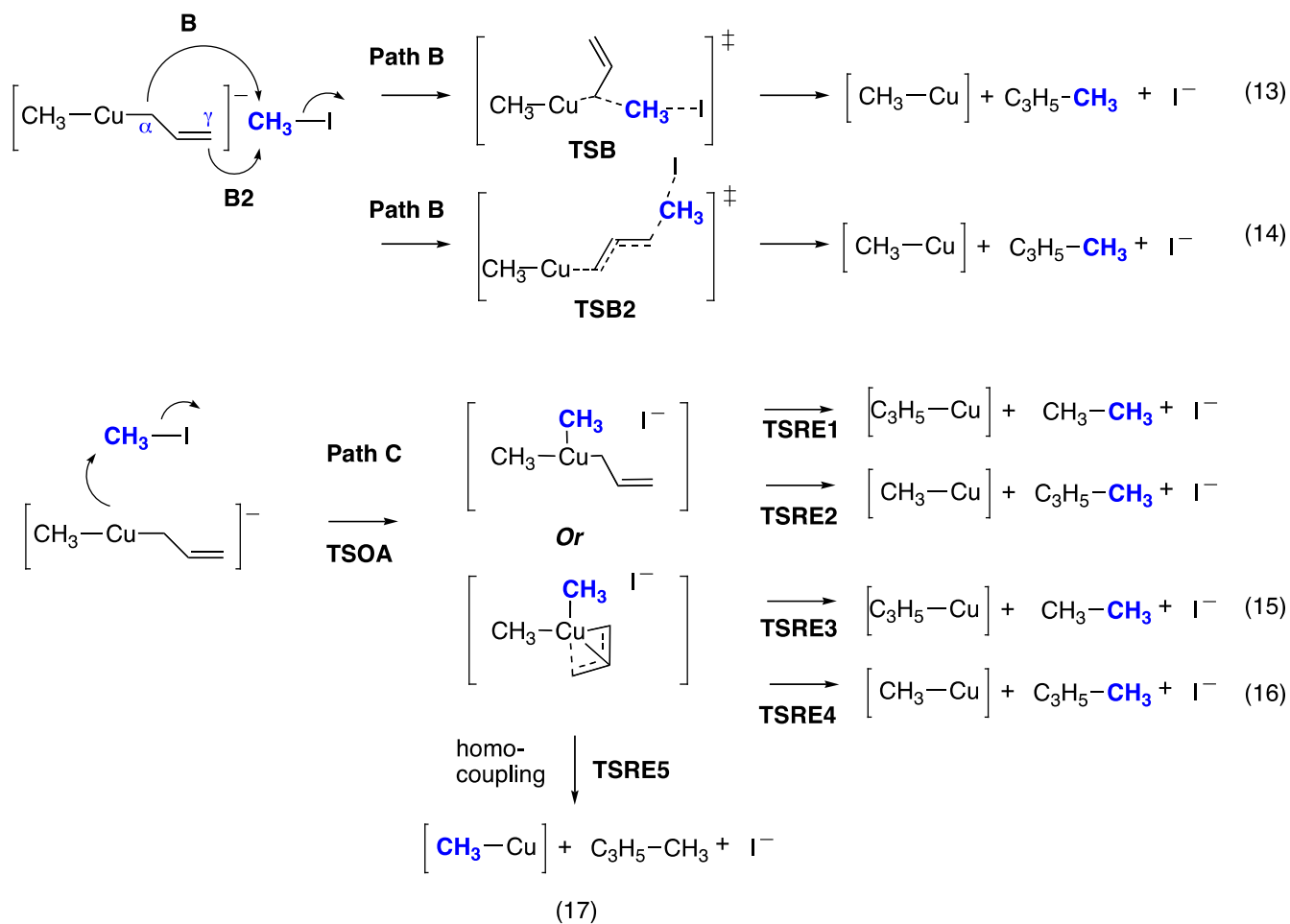
It is interesting to note that stable anionic 4-coordinate square planar Cu(III) complexes were not experimentally observed (c.f. Figure 1). Formation of these require the I⁻ to migrate from the T-shaped Cu(III) complex in Path C of Scheme 4 to take up a fourth coordination site (Scheme 4, eq. 10).⁴⁴ DFT calculations reveal that I⁻ migration within the IMC triggers reductive elimination from the T-shaped Cu(III) complex via **TSRE1** and **TSRE2**. However, IRC calculations reveal a tendency to connect the RE TSs to the anionic square-planar Cu(III) complexes. Thus, it is unclear if the 4-coordinate intermediate is formed and immediately undergoes RE, or if the TS is inclusive of the migration of I⁻ and RE, and occurs concertedly. The relative propensity to lose CH₃CH₃ versus RCH₃ via reductive elimination from 4-coordinate complexes has been previously examined experimentally and is essentially the same as that found via **TSRE1** and **TSRE2**.^{25,45}

Scheme 4. Potential reaction pathways for alkylation reactions of organocuprates, $[\text{CH}_3\text{CuR}]^-$ (**1-10**, Scheme 2) with methyl iodide (CH_3I).



An allyl ligand in the organocuprate (**9**, Scheme 2) allows for additional mechanistic scenarios. Path A (i.e. attack from the α -carbon of CH_3 , Scheme 4) is possible, but the $\text{S}_{\text{N}}2$ reaction may also take place from two nucleophilic positions on the allyl group (Scheme 5): Path B (α -carbon, eq. 13) or Path B2 (γ -carbon, eq. 14). For **9** in Path C, OA (**TSOA**) followed by **TSRE1** or **TSRE2** is possible, however coupling pathways via the Cu(III) intermediate are more numerous due to the possibility of higher denticity π -allyl intermediates (eqs. 15-17, Scheme 5).²³⁻²⁴

Scheme 5. Other reactive potential pathways accessible with an allyl (C_3H_5) ligand for allylic alkylation reactions of **9** (Scheme 2) with methyl iodide (CH_3I).



An examination of the predicted relative energies (Supporting information pages S8-S9, Table S6) for Paths A and B reveals that, with the exception of **TSB2** (γ -carbon of **9**, Scheme 5, eq. 14, -21.9 kJ mol $^{-1}$), the kinetic barriers for the S_N2 TSs **TSA** and **TSB** are always significantly above (by 32-42 kJ mol $^{-1}$ or more) the energy required for **TSOA** (Table 2). In addition, these kinetic barriers are approximately equal to (for cuprates **1-4** and **10**), or significantly above (for **5-9**) the energy of the separated reactants. Thus, mechanistic Paths A and B are not expected to occur under the near thermal

conditions of the ion-trap mass spectrometer. This is consistent with previous kinetic predictions for the ion-molecule reaction via an S_N2-like TS between dimethylcuprate and the electrophiles CH₃I^{22,20c} and C₃H₅I.²³ As the relative energies for Path C (Table 2, Schemes 4 and 5) are significantly lower than Path A and B in every case, Path C is expected to operate in all systems examined here. In addition, the source of experimentally observed I⁻ is most likely to be from Path C.

The energetics of **TSOA** for alkyl(methyl)cuprates bearing methyl, primary and secondary alkyl groups (**1-4**, Scheme 2) fall within a similar range (-41 to -44 kJ mol⁻¹), while *tert*-butyl(methyl)cuprate **5** is slightly higher (-40.2 kJ mol⁻¹). The trend in the energy of **TSOA** observed for the other R groups shows more variation. A higher energy of **TSOA** is required for methyl(phenethyl)cuprate **6** (-32.8 kJ mol⁻¹) and benzyl(methyl)cuprate **7** (-29.2 kJ mol⁻¹). For methyl(phenyl)cuprate **8**, the energy of **TSOA** is the highest of the species examined (-27.0 kJ mol⁻¹). Though less bulky than **6 – 8**, OA to allyl(methyl)cuprate **9** is also much higher in energy (-34.9 kJ mol⁻¹) than the alkylcuprates containing aliphatic carbon, while methyl(hydrido)cuprate **10** lies between the two trends (-38.7 kJ mol⁻¹). The energetic barriers follow the order alkyl << allyl ≈ PhCH₂CH₂ < PhCH₂ < Ph, in line with the relative ordering of the experimentally determined reaction rates and efficiencies. This agrees with the suggestion that OA is the rate-controlling step. The rate for methyl(hydrido)cuprate **10** lies outside this trend.

The preferred TS for reductive elimination is lower in energy than that of **TSOA** (by ~10 kJ mol⁻¹ or more for all species except dimethylcuprate **1**), indicating that reductive elimination is not the rate-limiting step. However, the competition between **TSRE1** and **TSRE2** in the reductive elimination step will determine the branching ratio (selectivity) for cross-coupling.

The energy of the TS for reductive elimination of ethane (**TSRE1**) shows only minor variation caused by the adjacent R group, with values between -39-54 kJ mol⁻¹. Not unexpectedly, the R group causes much greater explicit influence on the energy of the TS for reductive elimination of RCH₃ (**TSRE2**), which ranges from -33.9 kJ mol⁻¹ for **7** (R = PhCH₂) to -106.4 kJ mol⁻¹ for **10** (R = H)), the

latter TS of which is much lower in energy than the others, and explains the high selectivity for methane formation (cf. branching ratios, Table 1).

With regards to the allyl system, as mentioned above the reductive elimination from the intermediate complex of **9** is complicated by the π -allyl intermediate (Scheme 5, Path C). These intermediates open up the possibility of homo-coupling (Scheme 5, eq 17). The σ -type **TSRE1** will allow CH_3CH_3 formation to occur ($-51.9 \text{ kJ mol}^{-1}$), while the **TSRE4** (π -type) will allow $\text{C}_3\text{H}_5\text{-CH}_3$ formation to occur ($-42.0 \text{ kJ mol}^{-1}$). The pathways are competitive, but CH_3CH_3 formation should be preferred, as is experimentally observed (Table 1). Formation of $\text{C}_3\text{H}_5\text{-CH}_3$ via an σ -type TS is less competitive (**TSRE2**, $-36.7 \text{ kJ mol}^{-1}$), while the **TSRE3** (analogous TS to the homo coupling TS of Ref. 23) is not competitive with the other pathways ($-18.7 \text{ kJ mol}^{-1}$). The Cu(III) intermediate IMC is particularly stable ($-86.5 \text{ kJ mol}^{-1}$). The formation of this intermediate allows the original connectivity surrounding the copper to be lost, the methyl ligands become equivalent and **TSRE5** (which is the identical TS as **TSRE4**, $-42.0 \text{ kJ mol}^{-1}$) will result in homo-coupling (eq 17) of the allyl and methyl ligands originally bound to the cuprate.

Comparison of products of equation 3 and 4 shows that the formation of the RCH_3 is thermodynamically preferred in all cases except for **7** ($\text{R} = \text{PhCH}_2$) and **9** ($\text{R} = \text{C}_3\text{H}_5$), where RCu is more stable and thus CH_3CH_3 coupling is preferred (Supporting Information, Table S6).⁴⁶ For products formed via equation 1 and 2, RCH_3 formation is preferred for alkyl groups and $\text{R} = \text{H}$, while CH_3CH_3 formation is preferred for **6 – 9** (Table 2).

Table 2. Calculated B3LYP-D/Def2-QZVP//B3LYP/SDD:6-31+G(d) Energies (kJ mol^{-1}) of oxidative addition, intermediate species, reductive elimination and products for $[\text{CH}_3\text{CuR}]^-$ (Scheme 2) and CH_3I via Path C (Scheme 4 and 5).

	Cu(III) intermediates		separated products
--	-----------------------	--	--------------------

	TSOA	$[(\text{CH}_3)_2\text{CuR}]^-$ (*) eq 5	$[(\text{CH}_3)_2\text{ICuR}]^-$ eq 10	TSRE1	TSRE2	$\text{CH}_3\text{CH}_3 +$ $[\text{RCuI}]^-$ eq 11	$\text{CH}_3\text{R} +$ $[\text{CH}_3\text{CuI}]^-$ eq 12
1	-41.8	-44.7 (11.3)	-95.7	-43.0	-43.0	-278.5	-278.5
2	-44.2	-52.6 (-15.8)	-110.0	-46.8, -50.2 (f)	-60.1	-278.8	-295.7
3	-41.1	-46.2 (-10.5)	-107.5	-45.9	-54.7	-277.6	-288.0
4	-45.6, -44.0 (a)	-63.2 (-22.7)	-110.7, -108.2 (a)	-53.5, -50.7 (a)	-68.7, n/a (a)	-277.4	-300.4
5	-40.2	-55.3 (-19.9)	-90.9	-51.6	-60.8	-274.2	-292.6
6	-32.8	-34.0 (6.5)	-103.5	-44.6	-47.0	-272.8	-269.4
7	-29.2	-36.2 (-4.4)	-88.1	-48.3	-33.9	-263.3	-228.9
8	-27.0	-24.9 (n/a (b))	-78.9	-38.8	-36.2	-268.6	-251.3
9	-34.9	n/a	-89.8	-51.9	-36.7	-267.2	-243.0
		-86.5(-47.1) (c)	n/a	-18.7 (d)	-42.0 (e)		
10	-38.7	-40.2 (n/a (b))	-106.3	-39.0	-106.4	-284.2	-306.1

(*) Numbers in parenthesis refer to energy of separated products

(a) top side (first value) versus underside (second value) attack. See Supporting Information Scheme S1.

(b) neutral complex not stable.

(c) η -3 allyl Cu(III) intermediate.

(d) value for **TSRE3**, $\text{CH}_3\text{CH}_3 + [\text{RCuI}]^-$ formation via eq 15.

(e) **TSRE4**, **TSRE5**, $\text{CH}_3\text{R} + [\text{CH}_3\text{CuI}]^-$ formation via eq 16 or 17, where **TSRE4** = **TSRE5**.

As noted in Section 1.0, for R groups containing β -hydrogens, the primary product $[\text{RCuI}]^-$ appears to fragment to yield the secondary product ion $[\text{HCuI}]^-$ (eq. 6). Scheme 6 shows the mechanism for this β -hydride elimination reaction from $[\text{RCuI}]^-$; R = CH_3CH_2 , $\text{CH}_3\text{CH}_2\text{CH}_2$, $(\text{CH}_3)_2\text{CH}$, $(\text{CH}_3)_3\text{C}$, PhCH_2CH_2 , Ph and C_3H_5 , while Table 3 summarizes the energetics (relative to separated reactants CH_3I

and $[\text{CH}_3\text{CuR}]^-$) for each of the intermediates and transition states. It also highlights whether the reaction is experimentally observed. The results in Table 3 show that for the alkyl species ($\text{R} = \text{CH}_3\text{CH}_2$, $\text{CH}_3\text{CH}_2\text{CH}_2$, $(\text{CH}_3)_2\text{CH}$, and $(\text{CH}_3)_3\text{C}$) and $\text{R} = \text{PhCH}_2\text{CH}_2$ this is a facile elimination reaction, owing to a much lower barrier than the energy required for the preceding cross-coupling reaction (barriers are $\sim 40\text{-}65 \text{ kJ mol}^{-1}$ lower than **TSRE1**, Table 2). This is consistent with the observation of $[\text{HCuI}]^-$ in the mass spectrum of the reaction of $[\text{CH}_3\text{CuR}]^-$ with methyl iodide. Thus any of the $[\text{RCuI}]^-$ byproducts of the coupling reaction mentioned above may undergo this decomposition before they are collisionally cooled. For $\text{R} = \text{Ph}$, along with the TS barrier to β -hydride elimination being unfavorably high (-8.0 kJ mol^{-1}), the benzyne product is predicted to be well above the energy of the separated reactants ($108.8 \text{ kJ mol}^{-1}$) and thus this is not a viable decomposition pathway. This is consistent with β -hydride decomposition of $[\text{PhCuI}]^-$ not being observed (Figure 1c). $[\text{C}_3\text{H}_5\text{CuI}]^-$ is also predicted to be able to undergo β -hydride elimination, though this reaction is not as facile as for the saturated alkyl R groups, due to the thermodynamically unfavorable formation of allene.

Scheme 6. General reaction mechanism for β -hydride transfer and elimination from the product ions $[\text{RCuI}]^-$, with R groups possessing hydrogens in the β -position, R = CH_3CH_2 , $\text{CH}_3\text{CH}_2\text{CH}_2$, $(\text{CH}_3)_2\text{CH}$, $(\text{CH}_3)_3\text{C}$, PhCH_2CH_2 , Ph and C_3H_5 .

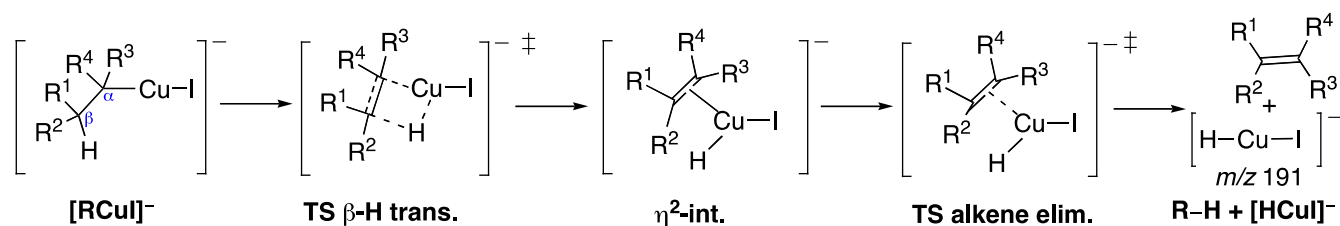


Table 3. Calculated B3LYP-D/Def2-QZVP//B3LYP/SDD:6-31+G(d) Energies (in kJ mol^{-1}) for β -hydride transfer and elimination for $[\text{CH}_3\text{CuR}]^-$ and CH_3I , where R = a group with β -H, i.e. decomposition of $[\text{RCuI}]^-$ (eq 6 and Scheme 6). All energies are relative to separated reactants $[\text{CH}_3\text{CuR}]^-$ (Scheme 2) and CH_3I .

R =	β -hydride transfer and elimination				separated products	observed?
	$[\text{RCuI}]^-$	TS β -H trans.	η^2 -int.	TS alkene elim.	R-H + $[\text{HCuI}]^-$ (eq 6)	
CH_3CH_2	-278.8	-107.0	-190.4	-191.7	-202.1	yes
$\text{CH}_3\text{CH}_2\text{CH}_2$	-277.6	-111.5	-196.1	-199.5	-206.2	yes
$(\text{CH}_3)_2\text{CH}$	-277.4	-100.8	-201.6	-205.0	-211.7	yes
$(\text{CH}_3)_3\text{C}$	-274.2	-92.3	n/a (a)	-204.2	-209.1	n/a
PhCH_2CH_2	-272.8	-109.8	-195.3	-197.6	-195.3	yes
Ph	-268.6	-8.0	-12.6	n/a (b)	108.8	no
C_3H_5	-267.2	-62.0	-113.3	-112.4	-126.3	yes

(a) no stable intermediate located, collapses into products.

(b) high energy reaction.

3.0 Comparison of R group effect on overall selectivity and reactivity.

Oxidative addition is controlled by the HOMO energy The oxidative addition of methyl iodide to dimethylcuprate affords the trimethylcopper(III) intermediate (Path C of Scheme 4 where R = CH₃), which has the ability to then undergo reductive elimination to yield a cross-coupled product, either with or without the presence of iodide. By replacing one of the identical methyl ligands with non-identical organic R group, the relative energy of addition of methyl iodide to the organocuprate is expected to vary due to both the electron donating ability and the steric bulk of the ligand, both of which influence the energy required for OA to occur. To examine these influences, we have plotted (Figure 3): (A) the TSOA; and (B) the HOMO energies of [CH₃CuR]⁻, as a function of R.

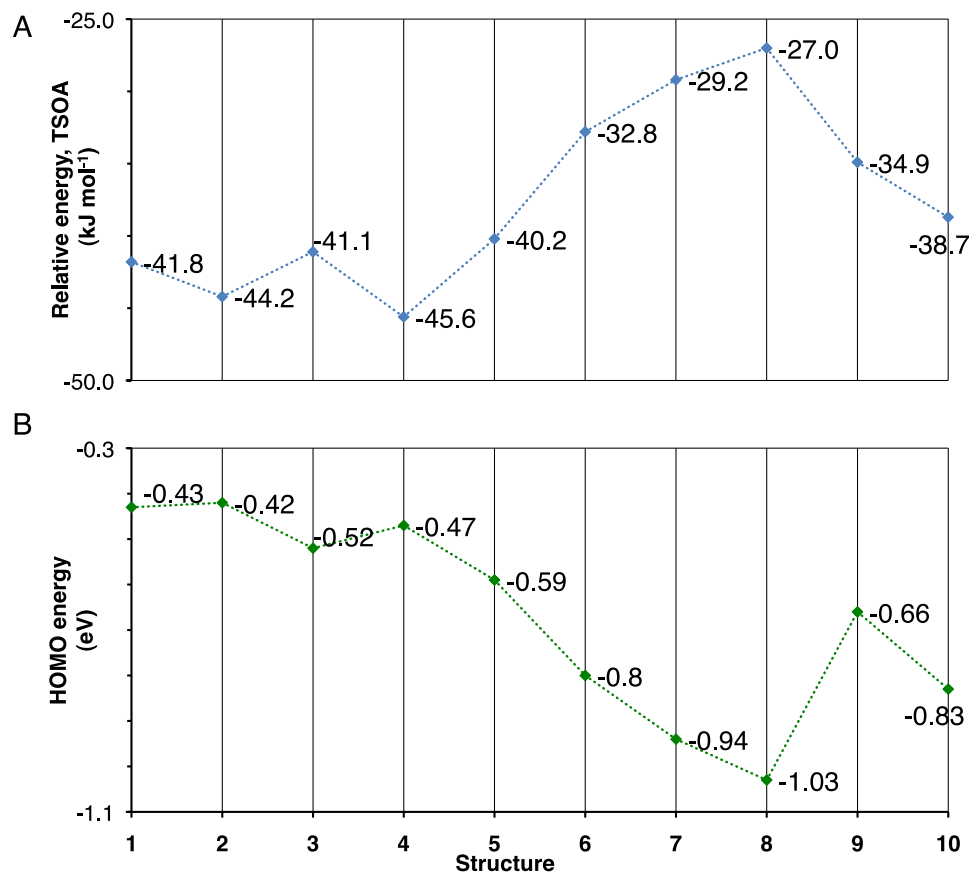


Figure 3. (A) Relative energy of transition state for the oxidative addition of methyl iodide to [CH₃CuR]⁻ (TSOA, kJ mol⁻¹), **1-10** (Scheme 2); (B) highest occupied molecular orbital (HOMO) energies (eV) calculated at optimization level for [CH₃CuR]⁻, **1-10** (Scheme 2).

An examination of Figure 3 (A) reveals that the activation energy required for oxidative addition increases with steric bulk and with inclusion of an unsaturated group in the ligand. For example, non-aliphatic R groups (i.e. **6** - **9**) require a higher activation energy. When R = H (**10**), the OA energy is slightly higher than R = CH₃ (by ~3 kJ mol⁻¹). One can see a correlation between the energy level of the highest occupied molecular orbital (HOMO) energy and the energy of the oxidative addition TS. That is, species that give similar relative energies for **TSOA**, also have similar HOMO levels. Thus, the organocuprates with lower HOMOs have higher barriers for oxidative addition. This is illustrated for **8** ([CH₃CuPh]⁻) which has the lowest lying HOMO (-1.03 eV) and the highest energy **TSOA** (-27.0 kJ mol⁻¹). An exception to this trend is R = H; though the **TSOA** is similar in energy as R = CH₃, the HOMO is much lower lying (-0.43 compared to -0.83 **1** and **10** respectively).

The relative barrier heights for reductive elimination control the coupling selectivity. An examination of Figure 4 reveals the role of **TSRE** in controlling the branching ratios of the two bond-coupling pathways (eq 11 and 12). Where formation of ethane (eq. 11, **TSRE1**) is experimentally observed in greater abundance, the **TSRE1** is lower in energy. Where RCH₃ is formed in greater abundance (eq 12), **TSRE2** is lower in energy. There is thus a good agreement between the predicted theoretical trends and experimentally determined branching ratios for the formation of [CH₃CuI]⁻ and [RCuI]⁻. When R = H, the **TSRE1** is particularly facile, (106.4 kJ mol⁻¹).

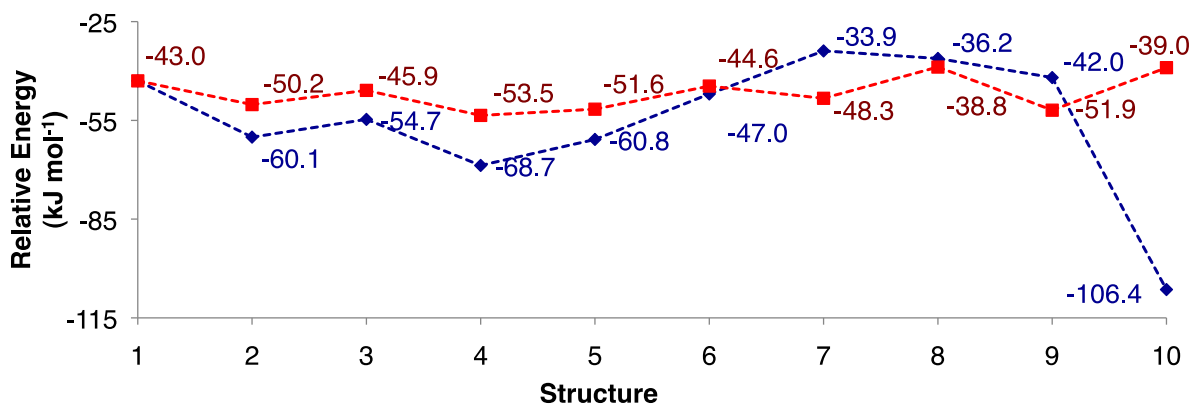


Figure 4. Relative energy of transition state for the reductive elimination at either ligand of methyl iodide to $[\text{CH}_3\text{CuR}]^-$ (kJ mol^{-1}), structures **1-10** (Scheme 2). Red points = **TSRE1**, blue points = **TSRE2**.

The structural effects of R on TSOA and TSRE. Taking the reaction of methyl(*n*-propyl)cuprate as a representative case, we show the structures of the key TSs, i.e., **TSOA**, **TSRE1** and **TSRE2**, in Figure 5. Table 4 summarizes the values for important bond lengths and angles for the key TSs for the whole series of cuprates (**1 – 10**).

The linear geometry of the cuprate species does not significantly change with R ligand in the **TSOA**. While *t*-butyl and phenylcuprates **5** and **8** become slightly bent ($169\text{-}170^\circ$), the R–Cu–CH₃ moiety of the other cuprates are almost linear ($173\text{-}174^\circ$). There is no apparent correlation between the OA energies, HOMO level and the bend from linearity required.

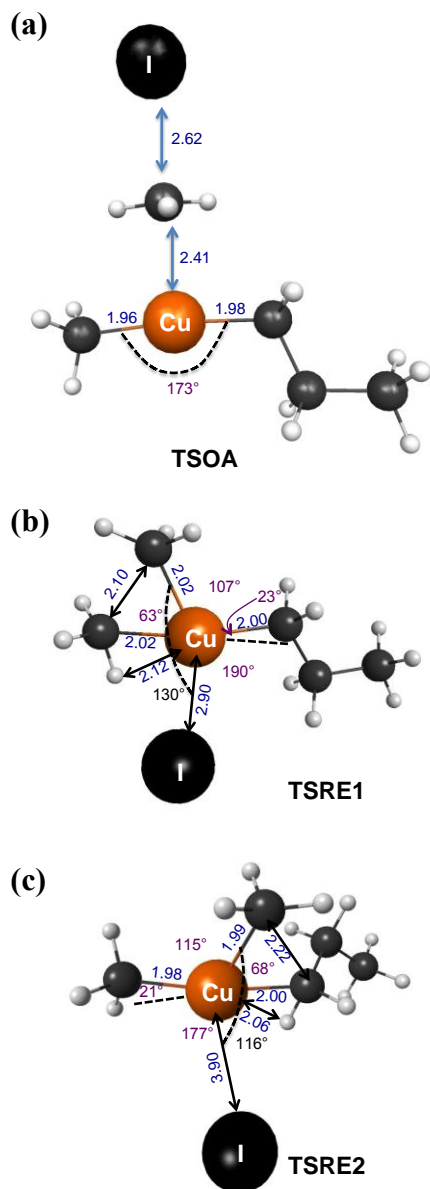


Figure 5. Key calculated TS structures, bond lengths (Å) and angles for **3**, $[\text{CH}_3\text{CuCH}_2\text{CH}_2\text{CH}_3]^- + \text{CH}_3\text{I}$: (a) **TSOA**; (b) **TSRE1**; and (c) **TSRE2** (Scheme 4, Table 5).

The **TSRE1** and **TSRE2** are influenced by the electron donating ability of the ligand^{26b} and the ability to deform the planar Cu complex structure. **TSRE2** is more directly affected by the nature of R (c.f. energies in Figure 4). While **TSOA** is trigonal planar, both RE TSs in this example are deformed tetrahedrally. This pyramidalization is brought about by the iodide atom interacting with the copper center (Figure 5 b and c). In the neutral RE TSs, where I^- is lost, this deformation is not observed, and

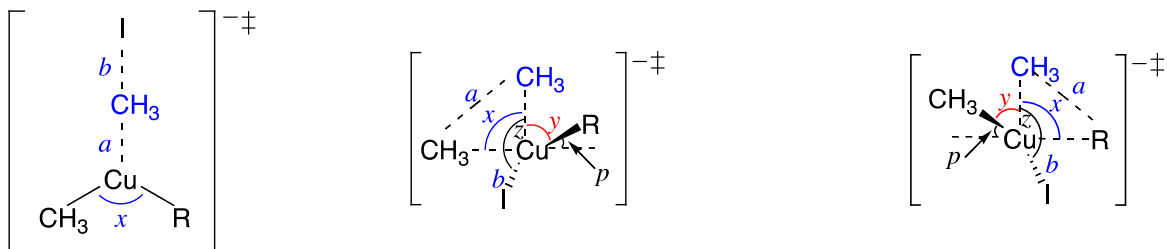
the TS is trigonal planar. Where the sterics of the R group allow for interaction of I⁻ with the copper, the RE barrier is substantially decreased. This type of deformation on the RE TS has been noted previously for the reaction of **1** with methyl iodide.^{20c}

The species which have an opportunity for agostic interaction at the open coordination site of the T-shaped copper(III) complex also have a lower energy **TSRE2**.

Regardless of the R group, **TSRE1** takes a similar tetrahedral geometry. The angle p (Table 5) refers to the dihedral angle created by the R carbon, Cu atom, cis-CH₃ carbon, and trans-CH₃ carbon, and shows the loss of planarity of these four atoms upon going from the T-shaped Cu(III) intermediate to the reductive elimination TS. This angle is between 22-25° for all R groups examined. This agrees with the similar relative **TSRE1** energy of all the species examined, i.e. there is little change in the TS with respect to changing the adjacent ligand.

In contrast, the corresponding angle, p , for **TSRE2** significantly depends on the R group. Not all of the R ligands examined allow I⁻ access to the copper center in the TS, in order to assist the deformation of the trigonal planar species. While the alkyl cuprates **2-4** undergo a similar degree of tetrahedral deformation in **TSRE2**, as is the case with dimethylcuprate **1** (with p between 21-22°), **TSRE2** for *t*-butyl(methyl)cuprate **5** remains trigonal planar ($p = 0^\circ$). Indeed, this species is an IMC with respect to the iodide atom, i.e. iodine is not interacting with the copper center (length Cu-I, $b = 5.80 \text{ \AA}$), but is stabilized by the agostic methyl group. The same planarity and lack of I⁻ interaction is true for methyl(benzyl)cuprate **7** ($b = 5.55 \text{ \AA}$, $p = 5^\circ$). Methyl(phenethyl)cuprate **6** also goes through a trigonal planar TS ($p = 5^\circ$) which is not tetrahedrally deformed, however there is some interaction between the iodide and the copper center ($b = 3.86 \text{ \AA}$). As such, **6** is an intermediate case between alkyl and Ph containing alkyl ligands. Since the bulk of the Ph group can limit access of the iodide to the copper center, the phenethyl group adopts a conformation in which the Ph group points away from the copper centre, and thus there is no opportunity for an agostic interaction. The case of methyl(hydrido)cuprate **10** is special, where the entire TS is quite planar and has a tighter angle between the bond forming atoms.

Table 4. Key bond lengths and angles for: (a) **TSOA**; (b) **TSRE1**; and (c) **TSRE2** (Scheme 4, Figure 5).



	TSOA			TSRE1						TSRE2					
	(Å)			(Å)						(Å)					
	<i>a</i>	<i>b</i>	<i>x</i>	<i>a</i>	<i>b</i>	<i>x</i>	<i>y</i>	<i>z</i>	<i>p</i>	<i>a</i>	<i>b</i>	<i>x</i>	<i>y</i>	<i>z</i>	<i>p</i>
1	2.41	2.63	174°	2.12	2.95	64°	111°	127°	22°	2.12	2.95	64°	111°	127°	22°
2	2.44	2.60	174°	2.11	2.94	63°	111°	129°	21°	2.22	3.11	68°	116°	115°	21°
3	2.41	2.62	173°	2.11	2.90	63°	107°	130°	23°	2.22	3.09	68°	115°	116°	21°
4(a)	2.45, 2.44	2.58, 2.59	173°, 173°	2.10, 2.11	2.90, 2.89	63°, 63°	109°, 108°	130°, 129°	22°, 24°	2.20, n/a	3.05, n/a	66°, n/a	111°, n/a	130°, n/a	22°, n/a
5	2.42	2.60	170°	2.11	2.89	63°	109°	129°	23°	2.26	5.80 (b)	67°	144°	n/a (b)	0°
6	2.36	2.66	173°	2.11	2.88	63°	107°	131°	23°	2.55	3.86	82°	111°	94°	5°
7	2.36	2.66	173°	2.11	2.81	63°	108°	137°	25°	2.25	5.55 (b)	69°	139°	n/a (b)	5°
8	2.30	2.70	169°	2.13	2.85	64°	108°	134°	25°	2.02	2.73	60°	100°	152°	22°
9	2.40	2.63	173°	2.09	2.80	62°	104°	140°	26°	(c)	(c)	(c)	(c)	(c)	(c)
10	2.37	2.64	173°	2.15	2.90	65°	109°	127°	25°	1.84	2.69	62°	103°	150°	0°

(a) First value is for topside attack, second for underside attack.

(b) not tetrahedrally coordinated to copper center as in the example in Figure 6, IMC.

(c) lowest energy RE for RCH₃ formation is not **TSRE2**, therefore no comparison is made.

Conclusions

“Organocuprate Complexity”⁹ arises from the fact that, in solution, the substrate,^{1,9} the counter cation, and the solvent⁴⁷ can all have an influence on reactivity.⁴⁸ In the gas-phase studies described above, this complexity has been reduced via the choice of the simple substrate methyl iodide and the absence of solvent and counter cation. Thus we have identified the intrinsic ligand effects of an R group on the reactivity and selectivity in C-C bond coupling of structurally related organocuprates, $[\text{CH}_3\text{CuR}]^-$.

In terms of overall reactivity, organocuprates containing alkyl R groups were found to be more reactive than those containing their larger, less saturated counterparts. The methyl(hydrido)cuprate, $[\text{CH}_3\text{CuH}]^-$ was found to be 8 times more reactive than dimethylcuprate $[\text{CH}_3\text{CuCH}_3]^-$, highlighting that copper hydrides are highly nucleophilic species. While R = PhCH_2 and Ph were less reactive, they were more selective in promoting CH_3CH_3 formation, which suggests they are intrinsically better “dummy” ligands. The allyl cuprate is both less reactive than the alkyl cuprates and less selective in the formation of the C-C bond coupling products, due to the possibility of isomerization and homo-coupling. This was shown by use of CD_3I , which revealed the presence of a homo-coupling product. Thus the allyl group is a poor dummy ligand.

An ongoing challenge in the use of Gilman reagents is that decomposition reactions can compete with the desired coupling reaction, thereby limiting the temperature range at which coupling reactions can be carried out. These decompositions also contribute to “Organocuprate Complexity”. A well known decomposition pathway involves β -hydride elimination⁴¹ to form copper hydrides,⁴⁹ which can undergo further reactions with the organic substrate.⁵⁰⁻⁵¹ Indeed independently generated copper hydrides are known to reduce alkyl halides.⁵¹ Our experimental results reveal a tendency for product ions with β -hydrogens to undergo β -hydride decomposition as a consequence of the high exothermicity associated with the reductive elimination step. In a synthetic reaction, this could produce an undesirable copper hydride byproduct, that might react further with the organic substrate to give unwanted organic byproducts. Our subsequent examination of the reactions of $[\text{CH}_3\text{CuH}]^-$ with methyl iodide show that these byproducts would indeed be extremely reactive when present, and thus not only does β -hydride

elimination hamper the reaction via break down and loss of valuable ligand, but also via loss of substrate through the favored C-H bond forming reaction. R = PhCH₂ and Ph would thus also be favorable dummy ligands due to the lack of decomposition and side-reactions.

The computational results also provided valuable insights into the ligand effects. An OA/RE pathway was found to be the lowest in energy for all species. OA controls the overall rate of reaction, while RE controls the selectivity of C-C bond coupling. With respect to the change in reactivity as a function of R: (1) the energetic barrier for OA is directly related to the HOMO level of the organocuprate reagent; while (2) RE is controlled by the ability of the R ligand to help deform the RE transition state. The agostic interaction, stability of Cu(III) intermediate and steric considerations were factors for the latter. The presence of a halide ion (I⁻) was found to be a key requirement for RE to occur, lowering the energy of pyramidalization required in the transition state. Sterics of certain R groups prevented this Cu-I interaction in some instances, but may offer enhanced stability. The exothermicity of the RE was found to be more than sufficient to fuel β-hydride elimination of [RCuI]⁻, in good agreement with the experimental observation of [HCuI]⁻. The observed homo-coupling with R = allyl was rationalized by the intermediacy of an η³-allyl Cu(III) intermediate. Thus our results support tuning of the HOMO level of the reagent to match that of the LUMO of the electrophile, whilst choosing ligands that allow pyramidalization during the RE and preventing, wherever possible, β-hydride elimination.

These results have implications for the choice of ligand for higher selectivity or efficiency and suggest that gas-phase studies can be used to screen and test the stability, intrinsic reactivity and selectivity of potential dummy ligands.

Tuning the “ease of transfer” or preventing decomposition are not the only benefits that might be realized with dummy ligands. Recent progress reveals sophisticated control over solvent effects and, in particular, counter ion placement, can also be achieved by tuning the dummy ligand.⁵² In some instances, ligands may even offer directing effects for the subsequent reactivity.⁵³ Clarity of mechanistic

understanding such as that gained from fundamental gas-phase studies will be vital to future efforts at achieving efficiency and selectivity in organocopper chemistry.

Acknowledgements:

We thank the ARC for financial support via grant DP110103844 (to RAJO) and through the ARC CoE program. NJR thanks: (i) The University of Melbourne Faculty of Science for a Science Faculty Scholarship; (ii) The University of Melbourne for a Postgraduate Overseas Research Experience Scholarship (PORES) to travel to the University of Tokyo; and (iii) the Global COE Program for Chemistry Innovation (MEXT, Japan) for partial support of the research in Tokyo. The Victorian Partnership for Advanced Computing (VPAC) and the Chemical Sciences High Performance Computing Facility (Gomberg) are acknowledged for generous provision of computational resources.

Supporting Information Available.

Complete citation for ref. 30. Cartesian coordinates, imaginary frequencies and energies (Hartrees) for species relevant to each of reaction pathways described in the text and full set at optimization level, including pre- and post- IMCs. Comparison table of M06 and B2PLYPD energies. This material is available free of charge via the Internet at <http://pubs.acs.org>.

References and footnotes

1. For monographs and reviews see: (a) *Modern Organocopper Chemistry*; Krause, N., Ed.; Wiley-VCH: Weinheim, Germany, 2002; (b) *The chemistry of organocopper compounds*; Rappoport, Z.; Marek, I. Eds.; Wiley: Chichester, UK, 2009; (c) Alexakis, A.; Bäckvall, J. E.; Krause, N.; Pàmies, O. Diéguez, M., *Chem. Rev.* **2008**, *108*, 2796–2823; (d) Harutyunyan, S.R.; den Hartog, T.; Geurts, K.; Minnaard, A.J.; Feringa, B.L., *Chem. Rev.* **2008**, *108*, 2824–2852; (e) Breit, B.; Schmidt, Y. *Chem. Rev.* **2008**, *108*, 2928–2951. For a recent issue devoted entirely to organocopper chemistry see: (f) *Organometallics*, **2012**, *31*, issue 22.
2. (a) Corey, E. J.; Posner, G. H. *J. Am. Chem. Soc.* **1967**, *89*, 3911-3912.
3. Modern synthetic approaches aim to reduce waste, thus the goal is not only to achieve selectivity, but also to be atom efficient, with the term “atom economy” being coined. See: Trost, B. M. *Science*, **1991**, *254*, 1471-1477.
4. Herein we refer to heteroleptic organocuprates which contain different (hetero) atom ligation as “heterocuprates” (for e.g. $[\text{CH}_3\text{CuSPh}]^-$), those with organometallic ligation to different organyl groups “mixed organocuprates” (for e.g. $[\text{CH}_3\text{CuPh}]^-$), and those with homoleptic organometallic ligation to the same groups “homocuprates” (for e.g. $[\text{CH}_3\text{CuCH}_3]^-$).
5. Corey, E. J.; Beames, D. J. *J. Am. Chem. Soc.* **1972**, *94*, 7210-7211.
6. (a) House, H.O.; Umen, M. J. *J. Org. Chem.* **1973**, *38*, 3893–3901; (b) Mandeville, W. H.; Whitesides, G. M. *J. Org. Chem.*, **1974**, *39*, 400–405; (c) House, H. O.; Chu, C. Y.; Wilkins, J. M.; Umen, M. J. *J. Org. Chem.* **1975**, *40*, 1460-1469; (d) Posner, G. H.; Whitten, C. E.; Sterling, J. J.; Brunelle, D. J. *Tetrahedron Lett.* **1974**, 2591-2594; (e) Corey, E. J.; Floyd, D.; Lipshutz, B. H. *J. Org. Chem.* **1978**, *43*, 3418-3420.

7. (a) Gorlier, J. P.; Hamon, L.; Levisalles, J.; Wagnon, J. *J. Chem. Soc., Chem. Commun.* **1973**, 88; (b) Posner, G. H.; Whitten, C. E.; Sterling, J. J. *J. Am. Chem. Soc.* **1973**, *95*, 7788-7800; (c) Posner, G. H.; Whitten, C. E. *Tetrahedron Lett.* **1973**, 1815-1818; (d) Bertz, S. H.; Dabbagh, G.; Villacorta, G. M. *J. Am. Chem. Soc.* **1982**, *104*, 5824-5826; (e) Bertz, S. H.; Dabbagh, G. *J. Chem. Soc. Chem. Commun.* **1982**, 1030-1032; (f) Bertz, S. H.; Eriksson, M.; Miao, G.; Snyder, J. P. *J. Am. Chem. Soc.* **1996**, *118*, 10906-10907.
8. (a) Erdik, E.; Ozkan, D., *J. Phys. Org. Chem.*, **2009**, *22*, 1148-1154; (b) Erdik, E.; Serdar, E. Z., *J. Organomet. Chem.*, **2012**, *703*, 1-8; (c) Erdik, E.; Ozkan, D., *Reac. Kinet. Mech. Cat.*, **2013**, *108*, 293-304; (d) Erdik, E.; Eroğlu, F.; Kalkan, M.; Pekel, O. O.; Özkan, D.; Serdar, E. Z., *J. Organomet. Chem.*, **2013**, *745-746*, 235-241.
9. Bertz, S. H.; Hardin, R.A.; Murphy, M. D.; Ogle, C. A.; Richter, J. D.; Thomas, A. A., *Angew. Chem. Int. Ed.*, **2012**, *51*, 2681–2685.
10. (a) Lipshutz, B. H.; Wilhelm, R. S.; Floyd, D. M. *J. Am. Chem. Soc.* **1981**, *103*, 7672-7674; (b) Lipshutz, B. H.; Wilhelm, R. S.; Kozlowski, J. A. *Tetrahedron* **1984**, *40*, 5005-5038; (c) Lipshutz, B. H. *Synthesis* **1987**, 325-341; (d) Lipshutz, B. H.; Sharma, S.; Ellsworth, E. L. *J. Am. Chem. Soc.* **1990**, *112*, 4032-4034; (e) Lipshutz, B. *Synlett* **1990**, 119-128; (f) Lipshutz, B. H.; James, B. *J. Org. Chem.* **1994**, *59*, 7585-7587.
11. (a) Bertz, S. H. *J. Am. Chem. Soc.* **1990**, *112*, 4031-4032; (b) Stemmler, T.; Penner-Hahn, J. E.; Knochel, P. *J. Am. Chem. Soc.* **1993**, *115*, 348-350; (c) Snyder, J. P.; Spangler, D. P.; Behling, J. R. *J. Org. Chem.* **1994**, *59*, 2665-2667; (d) Stemmler, T. L.; Barnhart, T. M.; Penner-Hahn, J. E.; Tucker, C. E.; Knochel, P.; Böhme, M.; Frenking, G. *J. Am. Chem. Soc.* **1995**, *117*, 12489-12497; (e) Barnhart, T. M.; Huang, H.; Penner-Hahn, J. E. *J. Org. Chem.* **1995**, *60*, 4310-4311; (f) Snyder, J. P.; Bertz, S. H. *J. Org. Chem.* **1995**, *60*, 4312-4313; (g) Bertz, S. H.; Miao, G.; Eriksson, M. *Chem. Commun.* **1996**, 815-816; (h) Mobley, T. A.; Müller, F.; Berger, S. *J. Am. Chem. Soc.* **1998**,

- 120, 1333-1334; (i) Boche, G.; Bosold, F.; Marsch, M.; Harms, K. *Angew. Chem. Int. Ed.* **1998**, *37*, 1684–1686; (i) Kronenburg, C. M. P.; Jastrzebski, J. T. B. H.; Spek, A. L.; van Koten, G. *J. Am. Chem. Soc.* **1998**, *120*, 9688-9689.
12. Krause, N. *Angew. Chem. Int. Ed.* **1999**, *38*, 79-81.
13. (a) Lipshutz, B. H.; Keith, J.; Buzard, D. J. *Organometallics* **1999**, *18*, 1571– 1574; (b) Putau, A.; Koszinowski, K. *Organometallics* **2010**, *29*, 3593-3601; (c) Putau, A.; Koszinowski, K. *Organometallics* **2010**, *29*, 6841-6842; (d) Putau, A.; Koszinowski, K. *Organometallics* **2011**, *30*, 4771-4778; (e) Putau, A.; Wilken, M.; Koszinowski, K. *Chem. Eur. J.*, **2013**, *19*, 10992-10999.
14. For an excellent review on the gas-phase chemistry of coinage metals see: Roithova, J.; Schroeder, D. *Coord. Chem. Rev.* **2009**, *253*, 666-677.
15. O'Hair, R. A. J. *Chem. Comm.*, **2006**, 1469 – 1481.
16. For a discussion on the differences between gas-phase and solution phase organometallic chemistry and their fruitful interplay see: Agrawal, D.; Schröder, D. *Organometallics*, **2011**, *30*, 32–35.
17. There is a growing use of MS to monitor organometallic reactions. See: (a) Henderson, W.; McIndoe, J. S., *Mass Spectrometry of Inorganic and Organometallic Compounds: Tools - Techniques - Tips*, John Wiley & Sons, Chichester, 2005; (b) *Reactive Intermediates. MS Investigations in Solution*; Santos, L.S.; Ed.; Wiley-VCH, Weinheim, 2010.
18. For mechanistic reviews of organocuprate chemistry from a theoretical perspective see: (a) Nakamura, E.; Mori, S. *Angew. Chem. Int. Ed.*, **2000**, *39*, 3751-3771; (b) Nakamura, E.; Yoshikai, N. *The chemistry of organocopper compounds*; Rappoport, Z.; Marek, I. Eds.; Wiley: Chichester, UK, 2009, Chapter 1, pp 1 – 21; (c) Mori, S.; Nakamura, E. In *Modern Organocopper Chemistry*; Wiley-VCH: Weinheim, Germany, 2002, Chapter 10, pp 315-346; (d) Yoshikai, N.; Nakamura, E. *Chem. Rev.*, **2012**, *112*, 2339-2372.

19. (a) Rijs, N.; Waters, T.; Khairallah, G. N.; O'Hair, R. A. J. *J. Am. Chem. Soc.*, **2008**, *130*, 1069-1079; (b) Rijs, N.J.; O'Hair, R. A. J. *Dalton Trans.*, **2012**, *41*, 3395-3406; (c) Vikse, K. L.; Khairallah, G. N.; McIndoe, J. S.; O'Hair, R. A. J. *Dalton Trans.*, **2013**, *42*, 6440 - 6449.
20. (a) Rijs, N.J.; Yates, B. F.; O'Hair, R. A. J. *Chem. Eur. J.* **2010**, *16*, 2674 - 2678; (b) Rijs, N. J.; O'Hair, R. A. J. *Organometallics* **2010**, *29*, 2282 – 2291; (c) Rijs, N.J.; Sanvido, G.B.; Khairallah, G.N.; O'Hair, R. A. J. *Dalton Trans.* **2010**, *39*, 8655 – 8662.
21. Rijs, N. J.; Brookes, N. J.; O'Hair, R. A. J.; Yates, B. F. *J. Phys. Chem. A* **2012**, *116*, 8910–8917.
22. James, P. F.; O'Hair, R. A. J. *Org. Lett.* **2004**, *6*, 2761–2764.
23. Rijs, N.J.; Yoshikai, N.; Nakamura, E.; O'Hair, R. A. J. *J. Am. Chem. Soc.* **2012**, *134*, 2569–2580.
24. Rijs, N. J.; O'Hair, R. A. J. *Organometallics* **2012**, *31*, 8012–8023.
25. Putau, A.; Brand, H.; Koszinowski, K. *J. Am. Chem. Soc.* **2012** *134*, 613-622.
26. (a) Nakamura, E.; Yamanaka, M. *J. Am. Chem. Soc.* **1999**, *121*, 8941-8942; (b) Yamanaka, M.; Nakamura, E. *J. Am. Chem. Soc.* **2005**, *127*, 4697-4706.
27. Waters, T.; O'Hair, R. A. J.; Wedd, A. G. *J. Am. Chem. Soc.* **2003**, *125*, 3384-3396.
28. The accuracy of these ion trap rate measurements was checked by measuring the known rate constant for the reaction: $\text{Br}^- + \text{CH}_3\text{I} \rightarrow \text{CH}_3\text{Br} + \text{I}^-$, which has been determined at room temperature previously in a flowing afterglow apparatus: (a) Gronert, S.; DePuy, C. H.; Bierbaum, V. M. *J. Am. Chem. Soc.* **1991**, *113*, 4009-4010. This rate was measured on the same day as each of the rate measurements for the reactions of methyl iodide with the organocuprates $[\text{CH}_3\text{CuR}]^-$. The previously reported $[\text{CH}_3\text{CuCH}_3]^- + \text{CH}_3\text{I}$ (ref. 22) and $[\text{CH}_3\text{CuCH}_3]^- + \text{C}_3\text{H}_5\text{I}$ (ref. 23) rate constants were also re-measured. In all cases the rate constants were reproduced within error limits. This close agreement shows that the ion trap provides reproducible ion-molecule rate constants of

near thermal ions, consistent with Gronert's equilibrium measurements, which have shown that ions within the ion trap are essentially at room temperature: (b) Gronert, S. *J. Am. Soc. Mass Spectrom.* **1998**, *9*, 845-848.

29. (a) Su, T.; Bowers, M.T. *Int. J. Mass Spectrom. Ion Phys.* **1973**, *12*, 347-356; (b) Lim, K.F. *Quantum Chem. Program Exch.* **1994**, *14*, 3.

30. Frisch, M. J.; et al. Gaussian 09, Revision C.01; Gaussian, Inc.: Wallingford, CT, 2010.

31. (a) Becke, A. D. *J. Chem. Phys.* **1993**, *98*, 5648-5652. (b) Lee, C.; Yang, W.; Parr, R. G. *Phys. Rev. B: Condens. Matter* **1988**, *37*, 785-789.

32. (a) Dolg, M.; Wedig, U.; Stoll, H.; Preuss, H. *J. Chem. Phys.* **1987**, *86*, 866-872; (b) Hariharan, P. C.; Pople, J. A. *Theor. Chim. Acta* **1973**, *28*, 213-222; (c) Clark, T.; Chandrasekhar, J.; Schleyer, P. V. R. *J. Comput. Chem.* **1983**, *4*, 294-301; (d) Krishnan, R.; Binkley, J. S.; Seeger, R.; Pople, J. A. *J. Chem. Phys.* **1980**, *72*, 650-654; (e) Gill, P. M. W.; Johnson, B. G.; Pople, J. A.; Frisch, M. J. *Chem. Phys. Lett.* **1992**, *197*, 499-505.

33. Yamanaka, M. Inagaki, A. Nakamura, E. *J. Comput. Chem.* **2003**, *24*, 1401-1409.

34. Although the structures and relative energies of loosely bound ion-molecule complexes (IMCs) are included in the Supporting Information for completeness (Table S5), the effectiveness of B3LYP in accurately predicting their properties was not assessed and they should therefore be treated with caution. However, these pre- and post-complexes do not influence the mechanistic conclusions drawn. Where intermediate Cu(III) intermediates and TS species are concerned, the energetic comparison of theoretical methods (B3LYP, M06 and B2PLYP-D, Supporting Information Table S1-4) was undertaken to ensure consistent mechanistic findings.

35. (a) Weigend, F.; Ahlrichs, R. *Phys. Chem. Chem. Phys.* **2005**, *7*, 3297-3305; (b) Weigend, F.; Furche, F.; Ahlrichs, R. *J. Chem. Phys.* **2003**, *119*, 12753-12762; Basis sets were obtained from the

- EMSL Basis Set Library *via* the Basis Set Exchange: (c) Schuchardt, K. L.; Didier, B.T.; Elsethagen, T.; Sun, L.; Gurumoorthi, V.; Chase, J.; Li, J.; Windus, T. L. *J. Chem. Inf. Model.* **2007**, *47*, 1045-1052; (d) Grimme, S. *J. Comp. Chem.* **2006**, *27*, 1787- 1799.
36. (a) Zhao, Y.; Truhlar, D. G. *Theor. Chem. Acc.* **2008**, *120*, 215-241; (b) Grimme, S. *J. Chem. Phys.* **2006**, *124*, 034108; (c) Schwabe T.; Grimme, S. *Phys. Chem. Chem. Phys.* **2007**, *9* 3397-3406.
37. Bode, B. M.; Gordon, M. S. *J. Mol. Graph. Model.* **1998**, *16*, 133-138.
38. Decarboxylation has also been used to generate organometallics in solution. For reviews on the formation of organometallics see: (a) Deacon, G. B. *Organomet. Chem. Rev., Sect. A* **1970**, *5*, 355-372; (b) Deacon, G. B.; Faulks, S. J.; Pain, G. N. *Adv. Organomet. Chem.* **1986**, *25*, 237-276. (c) Goossen, L. J.; Collet, F.; Goossen, K. *Isr. J. Chem.* **2010**, *50*, 617-629. For reviews on the use of catalytic decarboxylation reactions in synthesis see: (d) Gooßen, L. J.; Gooßen, K.; Rodriguez, N.; Blanchot, M.; Linder, C.; Zimmermann, B. *Pure Appl. Chem.* **2008**, *80*, 1725-1733; (e) Gooßen, L. J.; Rodriguez, N.; Gooßen, K. *Angew. Chem., Int. Ed.* **2008**, *47*, 3100-3120; (f) Weaver, J. D.; Recio, A.; Grenning, A. J.; Tunge, J. A. *Chem. Rev.* **2011**, *111*, 1846-1913; (g) Rodriguez, N.; Goossen, L. J. *Chem. Soc. Rev.* **2011**, *40*, 5030-5048; (h) Dzik, W. I.; Lange, P. P.; Gooßen, L. J. *Chem. Sci.* **2012**, *3*, 2671-2678; (i) Gooßen, L. J.; Gooßen, K. *Top. Organomet. Chem.* **2013**, *44*, 121-142.
39. For a recent demonstration of the reversibility of copper catalyzed carboxylation/decarboxylation see: Zhang, L.; Cheng, J.; Ohishi, T.; Hou, Z. *Angew. Chem. Int. Ed.* **2010**, *49*, 8670-8673.
40. O'Hair, R. A. J., In *Reactive Intermediates. MS Investigations in Solution*; Santos, L.S.; Ed.; Wiley-VCH, Weinheim, 2010, Chapter 6, pp 199 - 227.
41. For β -hydride transfer of organocopper compounds in solution see: (a) Whitesides, G.M.; Stedronsky, E.R.; Casey, C.P.; San Filippo, J. *J. Am Chem. Soc.* **1970**, *92*, 1426-1427; (b)

Whitesides, G.M.; Bergbreiter, D.E.; Kendall, P. E. *J. Am Chem. Soc.* **1974**, *96*, 2806 - 2813; (c) Miyashita, A.; Yamamoto, T.; Yamamoto, A. *Bull. Chem. Soc. Jpn.* **1977**, *50*, 1109-1117.

42. Previous computational chemistry calculations have highlighted that three coordinate organocopper (III) neutrals have a T shape and are unstable with respect to reductive elimination: (a) Dorigo, A. E.; Wanner, J.; Schleyer, P. V. *Angew. Chem. Int. Ed.* **1995**, *34*, 476-478; (b) Snyder, J. P. *J. Am. Chem. Soc.* **1995**, *117*, 11025-11026. This is consistent with the fact these species have remained experimentally elusive. Indeed organocopper (III) neutrals have only been characterized via NMR when they are stabilized via coordination to a fourth neutral ligand to give a square planar complex: (c) Bartholomew, E. R.; Bertz, S.H.; Cope, S.; Dorton, D. C.; Murphy, M.; Ogle, C.A. *Chem. Commun.* **2008**, 1176-1177; (d) Gärtner, T; Henze, W; Gschwind, R.M. *J. Am. Chem. Soc.* **2007**, *129*, 11362-11363. The role of high valent Cu species in organic reactions has generated renewed interest. For a review see: (e) Hickman, A. J.; Sanford, M. S., *Nature*, **2012**, *484*, 177-185.
43. For a related β -phenide transfer reaction in the gas-phase decomposition of $[\text{PhCH}_2\text{CH}_2\text{MgCl}_2]^-$ see: Khairallah, G. N.; Thum, C. C. L.; Lesage, D.; Tabet, J.-C.; O'Hair, R. A. J. *Organometallics*, **2013**, *32*, 2319–2328.
44. The predicted relative energies of these 4-coordinate Cu(III) species are somewhat lower than the energy of the separated reactants, as are barriers to OA and RE (see Table 3).
45. The mononuclear cuprates $[(\text{CH}_3)_3\text{CuR}]^-$ fragment to give both the coupling products RCH_3 and ethane, CH_3CH_3 (Scheme 1, E). The branching between these two fragmentation channels depends on the nature of the alkyl substituent R, the simple alkyl ligands (CH_3 , CH_3CH_2 and $\text{CH}_3\text{CH}_2\text{CH}_2$) being more prone to RCH_3 formation, the others groups being more prone to ethane formation. DFT calculations suggested that the reaction energetics for the reduction elimination of the RCH_3 product control this branching, as the energetics for ethane formation did not significantly vary as a function of R. The triple ions $[(\text{CH}_3)_6\text{Cu}_2\text{R}_2\text{Li}]^-$ also dissociate via formation of the coupling

product RCH₃ and the ethane coupling product CH₃CH₃ (Scheme 1, E), but do not give the RR homo-coupling product. On the basis of theoretical calculations, the prevalence of cross-coupling was rationalized by the preferential interaction of the central Li⁺ ion of the triple ions with two CH₃ groups of each [(CH₃)₃CuR]⁻ subunit, thereby blocking the homo-coupling channel. See Ref 25 for further detail.

46. The general order of stability of organocopper (I) neutrals is: alkynyl > alkenyl ≈ aryl > alkyl. See (a) van Koten, G.; Noltes, J.G. *Comprehensive Organometallic Chemistry*, Wilkinson, G.; Stone, F.G.A.; Abel, F.W. (Eds.), Pergamon Press, Oxford, 1984, Volume 2, 746-750; (b) van Koten, G.; James, S.L.; Jastrzebski, J.T.B.H.; *Comprehensive Organometallic Chemistry II*, Abel, F.W.; Stone, F.G.A.; Wilkinson, G. (Eds.), Pergamon Press, Oxford, 1995, Volume 3, 75-77.
47. In solution, lithium organocuprates can exist as solvent separated ion pairs (SSIP) or contact ion pairs (CIP). The latter are formed in solvents such as diethyl ether and show a higher reactivity. A further complication is that CIPs can undergo aggregation. For an excellent review that highlights these effects see: Gschwind, R. M., *Chem. Rev.*, **2008**, *108*, 3029–3053.
48. Complex equilibria between the different types of aggregation can also exist: Khiem, C. N. D.; Thach, L. N.; Iwasaki, T.; Kambe, N.; Boguslavskiy, A. A.; Pratt L. M. *J. Phys. Chem. A*, **2012**, *116*, 9027 – 9032.
49. For reviews on the reactions of copper hydrides see: (a) Riant, O. *The chemistry of organocopper compounds*; Rappoport, Z.; Marek, I. Eds.; Wiley: Chichester, UK, 2009, Chapter 15, pp 731 – 773; (b) Deutsch, C.; Krause, N.; Lipshutz, B. H. *Chem. Rev.* **2008**, *108*, 2916–2927.
50. (a) House, H. O.; DuBose, J. C. *J. Org. Chem.* **1975**, *40*, 788–790; (b) House, H. O.; and Umen, M. *J. Org. Chem.* **1973**, *38*, 3893-3901; (c) Johnson, C. R.; Herr, R. W.; Wieland, D. M. *J. Org. Chem.* **1973**, *38*, 4263-4268. (d) Scott, L. T.; Cotton, W. D. *Chem. Commun.*, **1973**, 320-321.

51. (a) Masamune, S.; Rossy, P. A.; Bates, G. S. *J. Am. Chem. Soc.* **1973**, *95*, 6452–6454; (b) Masamune, S.; Bates, G. S.; Georghiou, P. E. *J. Am. Chem. Soc.* **1974**, *96* 3686–3688; (c) Ashby, E. C.; Lin, J-J; Goel, A. B. *J. Org. Chem.* **1978**, *43*, 183–188.
52. For a recent example of sophisticated counter ion control using dummy ligands see: Vrancken, E.; Gérard, H.; Linder, D.; Ouizem, S.; Alouane, N.; Roubineau, E.; Bentayeb, K.; Marrot, J.; Mangeney, P. *J. Am. Chem. Soc.*, **2011**, *133*, 10790–10802.
53. For an example of a non-innocent ligand used to selectively pre-activate the C-H bond of a substrate prior to cupration, see: Komagawa, S.; Usui, S.; Haywood, J.; Harford, P. J.; Wheatley, A. E. H.; Matsumoto, Y.; Hirano, K.; Ryo, T.R.; Uchiyama, M. *Angew. Chem. Int. Ed.* **2012**, *48*, 12081 – 12085.

Table of contents graphic

